ALTERRA
WAGENINGEN UR

Heavy metal concentrations in the top soils of 'Achterhoek-Kreis Borken'

Mapping across the Dutch-German border

M. Knotters
D.J. Brus
A.H. Heidema

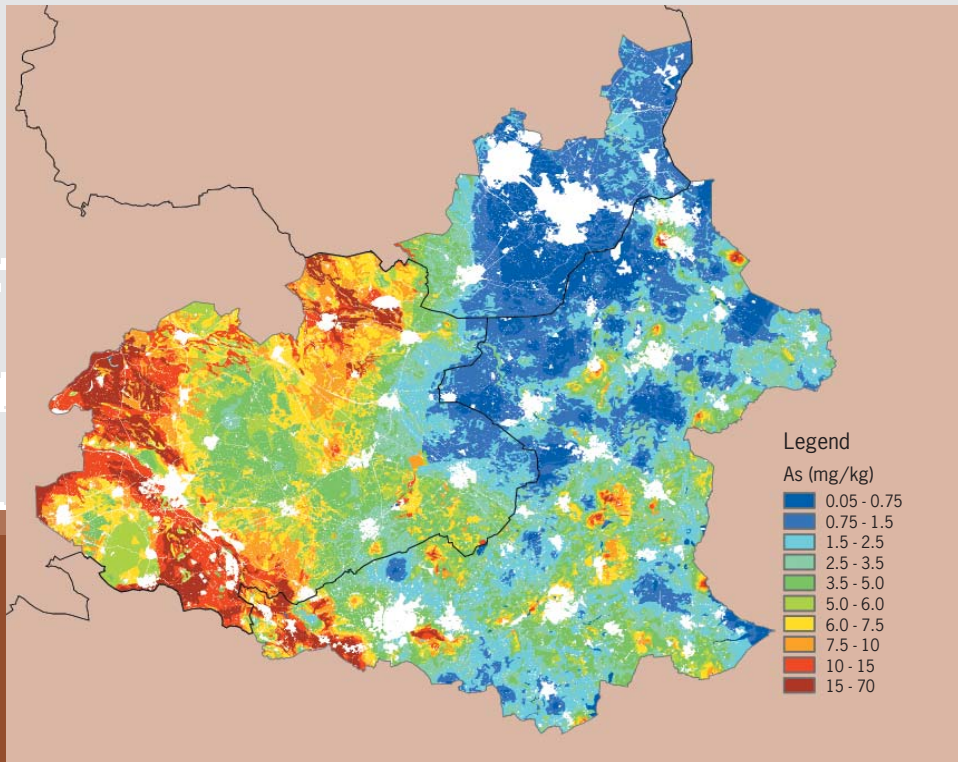

Alterra-rapport 1455, ISSN 1566-7197

provincie Gelderland
provincie Overijssel
provincie limburg
Ministerium für Umwelt und Naturschutz, Landwirtschaft und Verbraucherschutz des Landes Nordrhein-Westfalen
NRW.

Heavy metal concentrations in the top soils of 'Achterhoek-Kreis Borken'

By order of the Province of Gelderland

Heavy metal concentrations in the top soils of 'Achterhoek-Kreis Borken'

Mapping across the Dutch-German border

M. Knotters, D.J. Brus, A.H. Heidema

Alterra–Report 1455

Alterra, Wageningen, 2007

Martin Knotters, Dick Brus, Nanny Heidema, 2007. *Heavy metal concentrations in the top soils of 'Achterhoek-Kreis Borken'; Mapping across the Dutch-German border.* Wageningen, Alterra–Report 1455. 68 blz. 26 figs.; 5 tables; 9 refs.

Maps of concentrations on Arsenic, Cadmium, Copper, Lead, Nickel and Zinc are made for a Dutch-German border region. In the Dutch part of the area, heavy metal concentrations were measured at 113 locations and in the German part at 832 locations. For the Dutch part, spatially exhaustive ancillary information on clay content, organic matter content and pH is provided by the Dutch Soil Information System. For the German part, the Soil Map, 1:50,000, of Nordrhein-Westfalen provides spatially exhaustive information on clay content only. To obtain ancillary information on organic matter content and pH, point observations on organic matter content and pH are extrapolated by using the Soil Map, 1:50,000, of Nordrhein-Westfalen. Besides information on soil conditions, land use is an ancillary variable. The relationships between heavy metal concentrations and ancillary variables is described by multiple linear regression models, taking measurements below the detection limit into account by a maximum-likelihood procedure. Using these regression models, concentrations are predicted at a 25x25 m grid and next the regression residuals are interpolated spatially (Regression+Kriging). The accuracy of spatial predictions is evaluated by cross-validation.

Keywords: Arsenic, Cadmium, Copper, Lead, Nickel, Zinc, multiple linear regression, censored observations, left-censoring, Regression, Ordinary Kriging, cross-validation

ISSN 15667197

P.O. Box 47; 6700 AA Wageningen; The Netherlands
Phone: +31 317 474700; fax: +31 317 419000; e–mail: info@alterra.nl

[Alterra–Report 1455/April/2007]

Contents

Preface

The German state of Nordrhein-Westfalen and the Dutch provinces of Gelderland, Limburg and Overijssel co-operate in environmental protection for several years. Within the scope of this co-operation trans-border heavy metal concentrations in the top soil have been mapped for the area of Achterhoek, Twente and Kreis Borken, by order of the province of Gelderland. The results of this study are reported here. Concurrently, the institute IFUA-Projekt-GmbH in Bielefeld, Germany, mapped heavy metal concentration for the same region under the authority of the Landesamt für Natur, Umwelt und Verbraucherschutz (LANUV) Nordrhein-Westfalen in Esssen. The results of both studies will be compared. Since the same dataset is used in both studies, diverging results can only be explained from diverging methods.

In this interesting study we treated various soil data from Dutch and German sources. To interpret the German data set, knowledge of the German system of soil classification was needed. We are grateful to Dr. Gerald Krüger and Dr. Sandra Gommer of IFUA for their help in interpreting the German soil data. We express our gratitude to Ir. Stef Hoogveld, Ir. Kees Beurmanjer and Ir. Ben Schaap of the province of Gelderland for their helpful comments on an earlier version of this report. Dr. Luc Bonten (Alterra) is gratefully acknowledged for sharing his knowledge on the spatial distribution of heavy metal concentrations.

Wageningen, April 2007
Martin Knotters, Dick Brus, Nanny Heidema

Summary

Introduction
In the past, concentrations of heavy metals in the topsoil were mapped in the Netherlands and Germany following distinct methods, resulting in discontinuous patterns at the borderline. Besides methodological variation, differences between the Dutch and German datasets give further rise to discontinuous patterns. This study aims to eliminate methodological differences in mapping concentrations of heavy metals in the topsoil in the Dutch-German border district. Possible discontinuities along the borderline at the resulting maps will only be caused by differences between the Dutch and German data set. Regression is combined with kriging (Regression+Kriging). First, regression models are applied to predict concentrations deterministically from ancillary information on clay content, organic matter content, pH and land use. Next, the residuals of the regression models are interpolated by kriging. Concurrently with this study, concentrations of heavy metals have been mapped by the institute IFUA-Projekt-GmbH in Bielefeld, Germany, under the authority of the Landesamt für Natur, Umwelt und Verbraucherschutz (LANUV) Nordrhein-Westfalen in Esssen. Since the same data set is used, diverging results can only be explained from diverging methods.

Study area and dataset
The area is of about 304505 hectares, 162487 hectares of which are in the Netherlands and 142018 hectares in Germany. The German part has been sampled much more dense than the Dutch part (832 vs. 113 locations). Because of Dutch privacy law, for 65 % of the Dutch data set no spatial co-ordinates or only inaccurate spatial co-ordinates are available. These data are not used in the spatial interpolation of residuals. Only the remaining 35 % of data, with accurate spatial co-ordinates, are used in spatial interpolation. However, all data are used in regression analysis.

Regression analysis
For logarithmically transformed concentrations of Cadmium, Copper, Nickel, Lead and Zinc multiple linear regression models are fitted with clay content, organic matter content and pH as predictor variables. The models are fitted separately for agricultural land and natural areas including forests. For Arsenic only different intercepts are modeled for agricultural land and natural and forested areas, since the sources of Arsenic are not related to land use.
At about 10 % of the observations on Arsenic and 8 % of those on Cadmium is left-censored. These censored observations are taken into account in the regression analysis by applying a maximum-likelihood method for calibration.

Spatial interpolation
In Regression+Kriging the random function model is the sum of a deterministic

trend component and a stochastic component. The trend component is the part of heavy metal concentration that can be explained from predictor variables by the regression models. Information on these predictor variables has been made available for a 25x25 m grid. The stochastic component is the part of heavy metal concentration that cannot be explained from predictor variables. These residuals are calculated for the locations where the heavy metal concentrations have been observed. Next, the residuals are interpolated to the 25x25 m grid by ordinary kriging, and added to the deterministic predictions.
The accuracy of the spatial predictions can be calculated from the sum of the kriging variance of the kriged residuals and the variance of the expected value of (logarithmically transformed) heavy metal concentration. The kriging variance captures the residual variance of the regression model, the uncertainty as a result of spatial interpolation of residuals, and the errors of estimated values of predictor variables at the observation points.
The accuracy of the spatial predictions is evaluated by a cross-validation procedure. The prediction errors are summarized by the mean error as a measure of bias, the standard deviation of error as a measure of random error, and the root mean squared error, median absolute error and mean absolute error as measures of overall error.

Results

The percentages of variance accounted for varied from 3.8 % for the regression model of Copper in agricultural land to 61.6 % for the regression model of Lead in natural areas.
Spherical variograms were fitted to the residuals of Cadmium and Zinc, and nested spherical variograms were fitted to the regression residuals of Arsenic, Copper, Nickel and Lead.
None of the maps of the deterministic component of the heavy metal concentrations show discontinuities along the Dutch-German border. Adding interpolated residuals to these maps resulted in less smooth patterns. Also these final maps do not show discontinuities along the Dutch-German border.
The cross-validation results indicate that concentrations of Arsenic and Cadmium are systematically overestimated for the Dutch part of the study area. Concentrations of Arsenic, Cadmium and Zinc are predicted relatively precise for the Dutch part of the study area, i.e. relatively small random errors, and also relatively accurate, i.e. relatively small overall errors. Lead is predicted relatively inaccurate for the Dutch part. Copper and Nickel are predicted relatively accurate for the German part of the study area, as the median absolute error indicates.

Conclusions

1. Despite the fact that heavy metal concentrations are much more densely observed in Germany than in the Netherlands, the maps of heavy metal concentrations generally do not show pronounced discontinuities along the border;

2. Cross-validation generally does not indicate large differences in accuracy of spatial predictions between the German and Dutch part of the study area. However, the number of cross validation locations in the Dutch part is low and locations are clustered, which may result in inaccurate estimates of prediction errors;

3. The maps of prediction error variance show a clear discontinuity along the border: large prediction error variances in the Dutch part, small prediction

error variances in the German part. This is mainly explained by the kriging variance, which reflects the differences in density of observation points between the Dutch and the German part;

4. Lack of observed heavy metal concentrations in the Dutch part is compensated by relatively detailed ancillary information, resulting in maps without discontinuities along the German-Dutch border with respect to interpolated values. However, the variance of prediction errors is much larger in the Dutch part than in the German part, indicating that the predictions in the Dutch part are relatively inaccurate.

Chapter 1

Introduction

1.1 Background

The German state of Nordrhein-Westfalen and the Dutch provinces of Gelderland, Limburg and Overijssel co-operate in environmental protection for several years. Within the scope of this co-operation trans-border heavy metal concentrations in the top soil have been mapped for the area of Achterhoek, Twente and Kreis Borken, by order of the province of Gelderland. The results of this study are reported here. Concurrently, the institute IFUA-Projekt-GmbH in Bielefeld, Germany, mapped heavy metal concentration for the same region under the authority of the Landesamt für Natur, Umwelt und Verbraucherschutz (LANUV) Nordrhein-Westfalen in Esssen.

In the past, concentrations of heavy metals in the topsoil were mapped in the Netherlands and Germany following distinct methods, resulting in discontinuous patterns at the borderline. Besides methodological variation, differences between the Dutch and German datasets give further rise to discontinuous patterns. On one hand, the network of observations on heavy metal concentrations is much more dense in the German part than in the Dutch part of the study area. On the other hand, ancillary information on clay content, organic matter content and pH is more accurate for the Dutch part than for the German part of the study area. The maps constructed by the institute IFUA-Projekt-GmbH in Bielefeld, Germany, under the authority of the Landesamt für Natur, Umwelt und Verbraucherschutz (LANUV) Nordrhein-Westfalen in Esssen, are based on the same data set as in the study reported here. Therefore, diverging results can only be explained from diverging methods.

1.2 Aim

This study aims to eliminate methodological differences in mapping concentrations of heavy metals in the topsoil in the Dutch-German border district. One single method will be applied to both the Dutch and the German data set in a study area in the province of Gelderland and the state of Nordrhein-Westfalen. Since methodological differences are eliminated, possible discontinuities along the borderline at the resulting maps will only be caused by differences between the Dutch and German data set.

1.3 Outline

Study area and dataset are described in Chapter 2. The methodology followed in this study has two components: multiple linear regression and ordinary kriging. First, regression analysis is applied to a combined dataset of Dutch and German data resulting in models describing relationships between concentrations of heavy metals and ancillary information on land use and soil characteristics. The regression analysis is described in Chapter 3. Next, deterministic predictions of concentrations of heavy metals are made for locations of an exhaustive grid where information on the explanatory variables is available, and the regression residuals are interpolated to these grid locations by kriging. The interpolation errors are evaluated by cross-validation. The procedures of Regression+Kriging and cross-validation are described in Chapter 4. Chapter 5 summarizes the methods with a flowchart. Chapter 6 presents the results of the regression analysis. Chapter 7 shows the results of spatial interpolation. Chapter 8 ends with concluding remarks.

Chapter 2

Study area and dataset

2.1 Study area

Figure 2.1 shows the study area in the border district of the Netherlands and Germany. The area is of about 304505 hectares, 162487 hectares of which are in the Netherlands and 142018 hectares in Germany. The soil map, 1:50,000, of the Netherlands (Stiboka, 1975; Harbers and Rosing, 1983) provides information about the soil conditions in the Dutch part of the study area. The soil map, 1:50,000, of Nordrhein-Westfalen (Dworschak et al., 2001) summarizes the soil conditions of the German part of the study area.

Figure 2.1. Study area

2.2 Dataset

The sample locations are depicted in Figure 2.2. The German part has been sampled much more dense than the Dutch part (832 vs. 113 locations). Because of Dutch privacy law, for 65 % of the Dutch dataset no spatial co-ordinates or only inaccurate spatial co-ordinates are available. These data are not used in the spatial interpolation of residuals. The data of 40 locations with accurate spatial co-ordinates are used in spatial interpolation. The data of the complete set of 113 locations are used in regression analysis, however.

Table 2.1 summarizes the heavy metal concentrations in the top soils at sampled locations. In this study heavy metal concentrations are logarithmically transformed in the following way:

$$z = \log 10 \left(\frac{c}{c_{\mathrm{u}}} \right) ,$$

with c being the heavy metal concentration in mg/kg, and c_{u}=1 mg/kg.

Table 2.1. Summary of heavy metal concentrations in the top soil of agricultural land and natural areas including forests in the Transborder study area (after logarithmic transformation)

Heavy metal	agriculture		nature	
	mean	st.dev.	mean	st.dev.
Arsenic	0.5063	0.5902	0.5364	0.5377
Cadmium	-0.5899	0.2686	-1.082	0.6248
Copper	0.9404	0.2744	0.8495	0.4244
Lead	1.284	0.1680	1.632	0.3188
Nickel	0.6901	0.2960	0.6535	0.3644
Zinc	1.579	0.1940	1.312	0.4062

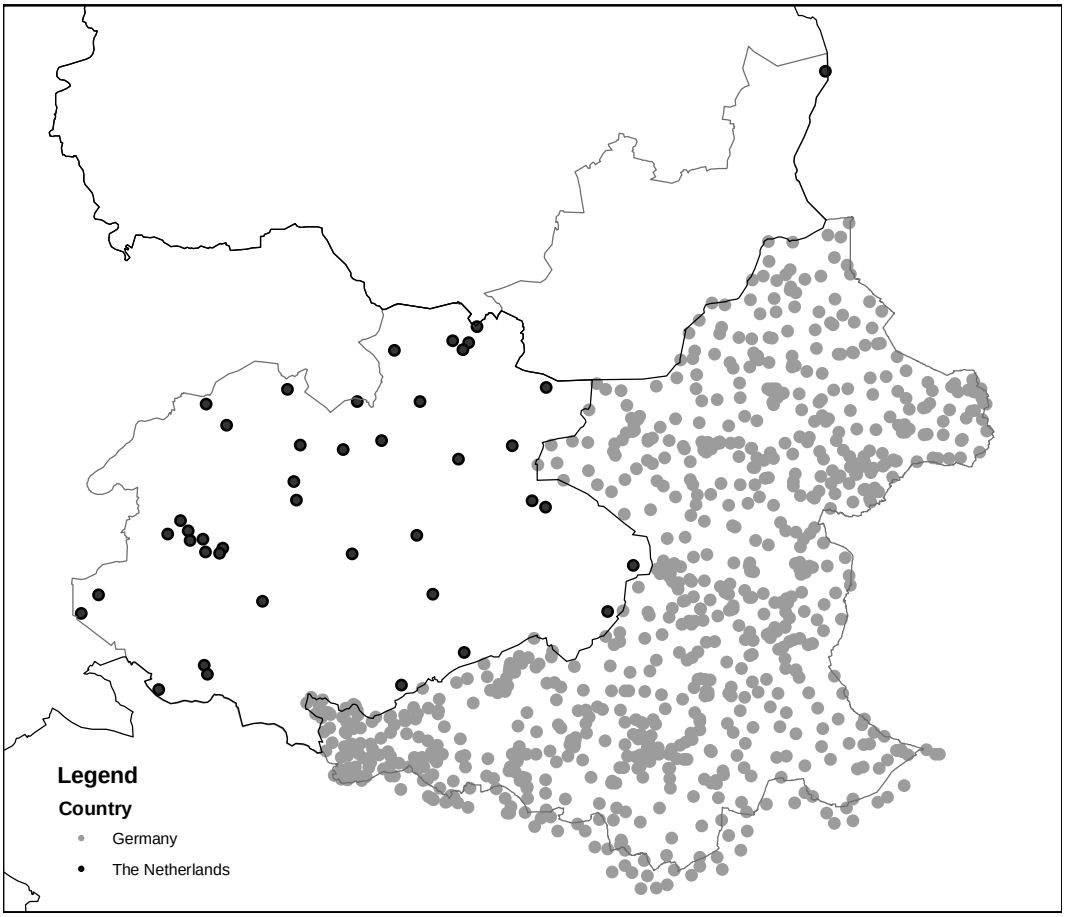

Figure 2.2. Sample locations: 40 in the Netherlands (dark dots), 832 in Germany (light dots). Note that in the Netherlands the spatial co-ordinates of many observation points are not available, for reasons of Dutch privacy law. Here, only locations with accurate co-ordinates are depicted

Chapter 3

Regression analysis

3.1 Model structures

For Cd, Cu, Ni, Pb and Zn distinct regression models were calibrated for agricultural land and natural areas including forests. The general structure of the model is

$$z = b_0 + b_0 * \log 10(CC + 0.1) + b_2 * \log 10(OM) + b_3 * pH_{\mathrm{CaCl_2}} + \varepsilon \ . \qquad (3.1)$$

The residual term ε has standard deviation s. c is the concentration of a heavy metal in the top soil. CC is the clay content (%), and OM is the percentage of organic matter. A value of 0.1 % is added to clay content to prevent for taking logarithms of zero values.
We used laboratory measurements of the predictor variables at the 113+832 sample locations (2.2) to calibrate the regression models. For Germany, OM has been calculated from the total organic carbon content (TOC) with $OM = 1.724 * TOC$. For the Netherlands, $pH_{\mathrm{pHCaCl_2}}$ was calculated from pH_{KCl} with

$$pH_{\mathrm{CaCl_2}} = -0.37 + 1.13 * pH_{\mathrm{KCl}} \ . \qquad (3.2)$$

In the Netherlands the clay content was determined by laboratory analysis. In Germany no laboratory measurements of clay content were available for the sample locations; clay contents were assigned to units of the soil map on the basis of field estimates.
For Arsenic distinction was made between natural and forested areas and agricultural land only with respect to the intercept of the regression line, since the sources of Arsenic are not related to land use. For As the following model was calibrated to the data:

$$\begin{aligned} lc \ &= \ b_0 + b_1 * nature + b_2 * \log 10(CC + 0.1) + b_3 * \log 10(OM) \\ &\quad + b_4 * pH_{\mathrm{CaCl_2}} + \varepsilon \ , \end{aligned} \qquad (3.3)$$

with land use class agricultural land being the reference level. The variable nature has zero value for locations in agricultural land and value 1 for locations in natural areas including forests.
First, the complete models given by Eqs. (3.1) and (3.3) were fitted to the data. Next, non-significant terms were dropped and the models were re-calibrated.

3.2 Censored observations

At about 10 % of the observations on As and at about 8 % of those on Cd is left-censored. For these censored observations we only know that the concentration is below a certain detection limit. Left-censored observations can be dealt with in naive ways such as by skipping them or by replacing them by the detection limit, half the detection limit, or zero. However, these approaches will result in biased estimates of regression coefficients. Therefore, we apply a maximum-likelihood method in calibrating regression models in the presence of censored observations of the response variable (Brus et al., 1992). The contribution of the non-censored values, c_{r}, to the deviance function is equal to

$$\begin{aligned} c_{\mathrm{r}} &= \log(2\pi s^2) + (z - b_0 - b_1 * nature - b_2 * \log 10(CC + 0.1) \\ &\quad -b_3 * \log 10(OM) - b_4 * pH_{\mathrm{CaCl_2}})^2 \ . \end{aligned}$$

The contribution of the censored values, c_{l}, to the deviance function is equal to

$$\begin{aligned} c_{\mathrm{l}} &= -2 \log\{\mathcal{N}[(z - b_0 - b_1 * nature - b_2 * \log 10(CC + 0.1) \\ &\quad -b_3 * \log 10(OM) - b_4 * pH_{\mathrm{CaCl_2}})/s]\} \end{aligned}$$

If the censored observations are replaced by the value of the detection limit r, then the function to be minimized is equal to

$$deviance = \sum [(z > \log 10(r)) * c_{\mathrm{r}} + (z \leq log10(r)) * c_{\mathrm{l}}] \ .$$

Note that the above function allows for various detection limits. This might be the case if measurement devices with various precisions have been applied.

Chapter 4

Spatial interpolation

4.1 Regression+Kriging

In Regression+Kriging the random function model is the sum of a deterministic trend component and a stochastic component:

$$Z(\mathbf{u}) = m(\mathbf{u}) + R(\mathbf{u}) \; . \tag{4.1}$$

The trend component is the part of heavy metal concentration that can be explained from predictor variables by the regression models given in Chapter 6. Information on these predictor variables has been made available for a 25×25 m grid as described in Section 4.2. Using this information, deterministic predictions of the heavy metal concentrations are made for a 25×25 m grid.

The stochastic component is the part of heavy metal concentration that cannot be explained from predictor variables by the regression models given in Chapter 6. This residual term is calculated from the difference between observed heavy metal concentrations and deterministic predictions by using the information for a 25×25 m grid as described in Section 4.2. These residuals are calculated for the locations where the heavy metal concentrations have been observed. Next, the residuals are interpolated to the 25×25 m grid by Ordinary Kriging using the software of GSLIB (Deutsch and Journel, 1998) and added to the deterministic predictions.

4.2 Deterministic predictions

Deterministic predictions are made for a 25×25 m grid, using information on the predictor variables of the regression models given in Chapter 6. This information is derived as follows.

The Netherlands

- clay content (CC), organic matter content (OM): median values for map units of the Soil Map 1:50,000, derived from the Dutch Soil Information System (Van der Pouw and Finke, 1999) and logarithmically transformed;

- $pH_{\mathrm{CaCl_2}}$: median values for map units of the Soil Map 1:50,000, derived from pH_{KCl} measurements in the Dutch Soil Information System (Van der Pouw and Finke, 1999), by using Eq. (3.2);
- land use: derived from the LGN4 database.

Germany

- clay content: estimates for map units of the Soil Map 1:50,000, provided by the Geologischer Dienst Nordrhein-Westfalen (Dworschak et al., 2001).
- organic matter content (OM), $pH_{\mathrm{CaCl_2}}$: values of $\log 10(OM)$ and $pH_{\mathrm{CaCl_2}}$, observed at points, were assigned to map units by averaging within map units. Values were extrapolated to non-sampled map units by clustering similar map units, using the German system of soil classification as described by Benzler et al. (1982) and summarized by Dworschak et al. (2001).
- land use: derived from a GIS database provided by IFUA-Projekt-GmbH.

Appendix A shows maps of clay content, organic matter content and pH, constructed in the way described before. Note the discontinuities along the border at the maps of organic matter content and pH. The information on predictor variables was transformed into deterministic predictions of heavy metal concentrations for each cell of the 25×25 m grid by the models given in Chapter 6.

4.3 Spatial interpolation of the residual term

It is important to note that two types of residuals can be distinguished. The first type of residuals remains after fitting the models to the observations at individual points, as described in Chapter 3. This first type of residual is not considered in the spatial interpolation. The second type of residuals, which are considered in the interpolation procedure, are the differences between observed and deterministically predicted heavy metal concentrations at the 25×25 m grid, based on information of the predictor variables as described in Section 4.2:

$$r(\mathbf{u}_i) = z(\mathbf{u}_i) - \tilde{z}(\mathbf{u}_i) \ , \tag{4.2}$$

where $z(\mathbf{u}_i)$ is the observed logarithmically transformed heavy metal concentration, and $\tilde{z}(\mathbf{u}_i)$ is the predicted logarithmically transformed heavy metal concentration at the observation points $\mathbf{u}_i$. Appendix B.1 shows schematically the procedure of adding interpolated residuals to deterministic predictions of Arsenic.

4.4 Accuracy of spatial predictions

Let $\epsilon(\mathbf{u}_j)$ be the difference between the interpolated and true value of logarithmically transformed heavy metal concentration at an interpolation point $\mathbf{u}_j$. The accuracy of the spatial predictions is quantified by the variance of $\epsilon(\mathbf{u}_j)$ which can be calculated from the sum of two components:

1. the kriging variance $\sigma^2_{\mathrm{K}}(\mathbf{u}_j)$;

2. the variance of the expected value of (logarithmically transformed) heavy metal concentration, $\sigma^2\{\mathrm{E}z(\mathbf{u}_j)\}$:

$$\sigma^2_\epsilon(\mathbf{u}_j) = \sigma^2_\mathrm{K}(\mathbf{u}_j) + \sigma^2\{\mathrm{E}z(\mathbf{u}_j)\} \ .$$

The kriging variance captures the residual variance of the regression model, the uncertainty as a result of spatial interpolation of residuals, and the errors of estimated values of predictor variables at the observation points. Appendix B.2 shows a scheme of the procedure followed in mapping the accuracy of spatial predictions.

4.5 Backtransformation to the original scale

The spatial predictions at a logarithmic scale are transformed to the original scale by

$$\tilde{c}(\mathbf{u}_j) = 10^{\tilde{z}(\mathbf{u}_j)} \ . \tag{4.3}$$

In contrast to the approach of lognormal kriging as described by Journel and Huijbregts (1978) (p. 570), we do not assumptions on a lognormal distribution of the original data. The straightforward way of backtransformation by Eq. (4.3) results in *median* unbiased estimates of concentrations of heavy metals at the original scale (De Oliveira, 2006). Given the skewed distributions of concentrations of heavy metals, the median is an appropriate measure of centrality.

4.6 Cross-validation procedure

The accuracy of the spatial predictions is evaluated by a cross-validation procedure. In this procedure, one of the n observation points is left out, and a spatial prediction for this point is made by using the remaining $n-1$ observation points. This is repeated until predictions were made for all n points. Next, the predictions are evaluated by calculating prediction errors and cross-validation measures.

The prediction error is the difference between the observed and predicted value at a cross-validation point:

$$e(\mathbf{u}_i) = z(\mathbf{u}_i) - \tilde{z}(\mathbf{u}_i) \ , \tag{4.4}$$

with $i, i = 1 \ldots n$ indicating the observation points and $z(\mathbf{u}_i)$ and $\tilde{z}(\mathbf{u}_i)$ indicating the observed and interpolated value at location $\mathbf{u}_i$, respectively. For cross-validation at the original scale, the values of $z(\mathbf{u}_i)$ and $\tilde{z}(\mathbf{u}_i)$ are backtransformed by Eq. (4.3).

The following cross-validation measures are calculated from the prediction errors.

- the mean error as a measure of systematic error or bias,

$$\mathrm{ME} = \frac{1}{n}\sum_{i=1}^{n} e(\mathbf{u}_i) \ ;$$

- the standard deviation of error as a measure of random error,

$$\mathrm{SDE} = \sqrt{\frac{1}{n-1}\sum_{i=1}^{n}\{\mathrm{ME} - e(\mathbf{u}_i)\}^2} \ ;$$

- the root mean squared error as a measure of overall error,

$$\text{RMSE} = \sqrt{\frac{1}{n}\sum_{i=1}^{n} e^2(\mathbf{u}_i)} \; ;$$

- the median absolute error (MEDAE) and mean absolute error (MAE) as measures of overall error that are less sensitive to outlying values than the RMSE.

The inverse of SDE is a measure of precision, the inverse of RMSE, MEDAE and MAE are measures of accuracy or overall resemblance of predictions with reality.

Chapter 5

Summary of methods

Figure 5.1 summarizes the methods applied in this study. Regression models are calibrated on the most accurate information being available. Next, the calibrated regression models are applied to make deterministic predictions of concentrations of heavy metals, using exhaustive information on the explanatory variables in a 25x25 m grid. Residuals are calculated for the locations where observations on heavy metal concentrations are available. These residuals are interpolated to the 25x25 m grid and added to the deterministic predictions. This results in maps of heavy metal concentrations.

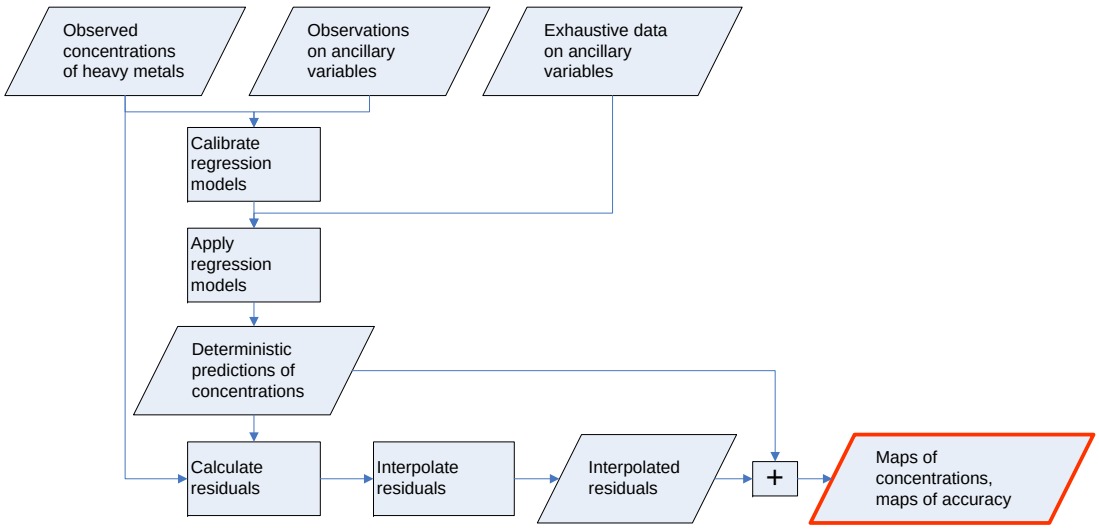

Figure 5.1. Flowchart of methods

Chapter 6

Results of regression analysis

Appendix C provides detailed information of the calibrated regression models, the percentages of variance accounted for and maximum-likelihood estimates of concentrations of heavy metals below the detection limit. Table 6.1 summarizes the regression models.

Table 6.1. Summary of regression models. Significant terms are indicated with + (only positive significant terms were selected). % of v.a.c.: percentage of variance accounted for

response variable	natural areas including forests				agricultural land			
	$\log 10(CC)$	$\log 10(OM)$	pH	% of v.a.f.	$\log 10(CC)$	$\log 10(OM)$	pH	% of v.a.f.
log10(As)	+*			9.7*	+*			9.7*
log10(Cd)		+	+	49.4		+	+	60.0
log10(Cu)	+	+		28.2	+	+		3.8
log10(Ni)	+	+	+	36.3	+		+	26.5
log10(Pb)	+	+		61.6	+	+		24.9
log10(Zn)	+	+	+	57.4	+	+	+	39.5

*) For As one model was calibrated

For Cu, Ni, Pb, and Zn, models showed a better fit in natural areas than in agricultural land, in terms of the percentage of variance accounted for. Note the poor fit of the model for Cu in agricultural land (3.8 % of variance accounted for).

Chapter 7

Results of spatial interpolation

7.1 Spatial structure of the stochastic model component

7.1.1 The variogram model

Sample variograms were calculated using the program GAMV of GSLIB (Deutsch and Journel, 1998). Next, spherical models were fitted to the sample variograms. The structure of a nested spherical model is

$$\begin{aligned}
\gamma_1(h) &= \begin{cases} c_0 + c_1 \cdot \left[1.5\frac{h}{a_1} - 0.5\left(\frac{h}{a_1}\right)^3\right] , & \text{if } h \le a_1 \\ c_0 + c_1 , & \text{if } h \ge a_1 \end{cases} \\
\gamma_2(h) &= \begin{cases} c_2 \cdot \left[1.5\frac{h}{a_2} - 0.5\left(\frac{h}{a_2}\right)^3\right] , & \text{if } h \le a_2,\ a_2 > a_1 \\ c_2 , & \text{if } h \ge a_2 \end{cases} \\
\gamma(h) &= \gamma_1(h) + \gamma_2(h)
\end{aligned} \tag{7.1}$$

7.1.2 Results of variogram modelling

Table 7.1 presents the fitted parameters of the semivariograms. Figure 7.1 shows the semivariograms.

Table 7.1. Parameter estimates of the double-spherical semivariograms for residuals between observed concentrations of heavy metals and predictions by regression models. c_0: nugget variance; c_1, c_2: partial sill variance; a_1, a_2: range

Heavy metal	Parameters of the semivariogram model for residuals				
	$\hat{c}_0$	$\hat{c}_1$	$\hat{a}_1$	$\hat{c}_2$	$\hat{a}_2$
Arsenic	0.049	0.117	1.916	0.041	18.149
Cadmium	0.025	0.068	1.509	-	-
Copper	0.011	0.047	0.785	0.016	7.790
Nickel	0.035	0.027	1.894	0.047	121.391
Lead	0.011	0.011	1.564	0.008	6.997
Zinc	0.022	0.037	3.984	-	-

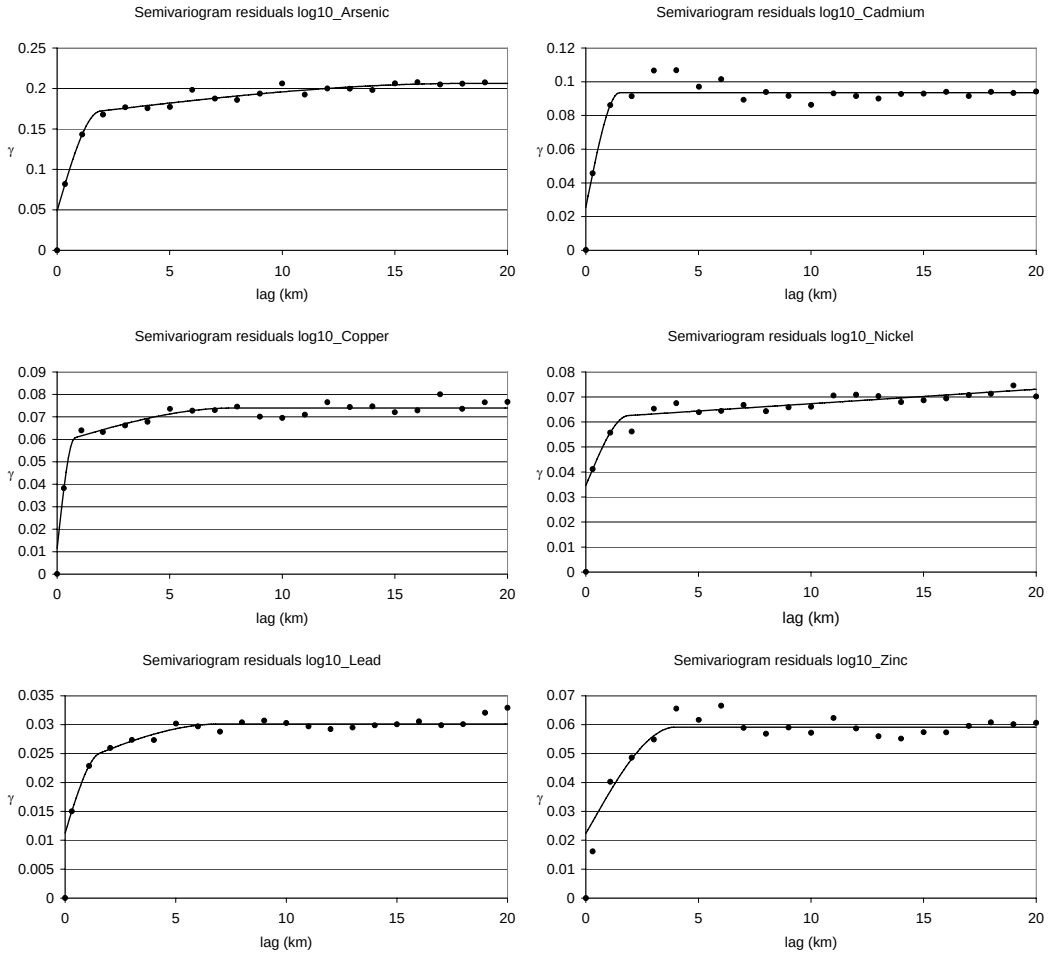

Figure 7.1. Semivariograms for the residuals between observed concentrations of heavy metals and predictions by regression models

7.2 Results of spatial interpolation

Appendix D shows maps of heavy metal concentrations, after being corrected with interpolated regression residuals, i.e., Regression+Kriging. Both maps of predictions at the logarithmic scale and the original scale are presented. The procedure of backtransformation is described in Section 4.5. In general the maps do not indicate pronounced discontinuities along the border. Discontinuities along the border are most pronounced at the maps of predicted concentrations of Cd and Cu at the original scale.

Appendix E gives maps of the variance of prediction errors at the logarithmic scale, calculated following the procedure described in Section 4.4. The maps show pronounced discontinuities along the border.

Table 7.2 shows the results of cross-validation at logarithmic scale. The mean error (ME) is a measure of systematic error. Concentrations of Arsenic and Cadmium are systematically underestimated for the Dutch part of the study area. The standard

deviation of error (SDE) summarizes the random errors and its inverse value is a measure of precision. The SDE values indicate that concentrations of Arsenic, Cadmium and Zinc are predicted more precisely for the Dutch part of the study area than for the German part. However, predictions of concentrations of Lead appear to be relatively imprecise in the Dutch part. Both the RMSE and the MAE reflect the overall prediction error (both systematic and random), the MAE being less sensitive to extreme values than the RMSE. The inverse values of RMSE and MAE are measures of accuracy, i.e. the overall resemblance of predictions with reality. The RMSE values indicate that concentrations of Arsenic, Cadmium and Zinc are predicted relatively accurate for the Dutch part of the study area. However, the RMSE indicates that predictions of Lead concentrations are relatively inaccurate in the Dutch part. The MAE indicates that concentrations of Copper and Nickel are predicted relatively accurate in the German part of the study area.

It should be noted that the number of cross-validation locations in the Dutch part is very low (40). Furthermore, about 14 locations are clustered. This may give rise to an inaccurate estimate of prediction errors in the Dutch part of the study area.

Table 7.2. Results of cross-validation at log10-scale. ME=mean error, SDE=standard deviation of error, RMSE=root mean squared error, MEDAE=median absolute error. D=Germany, NL=The Netherlands

Heavy	ME			SDE			RMSE			MEDAE		
metal	D	NL	tot.	D	NL	tot.	D	NL	tot.	D	NL	tot.
Arsenic	-0.02	0.11	-0.01	0.42	0.34	0.42	0.42	0.36	0.42	0.23	0.18	0.23
Cadmium	-0.00	0.04	-0.00	0.31	0.24	0.31	0.31	0.24	0.31	0.16	0.12	0.15
Copper	0.00	0.02	0.00	0.26	0.27	0.26	0.26	0.26	0.26	0.15	0.19	0.15
Lead	0.00	0.01	0.00	0.17	0.20	0.17	0.17	0.20	0.17	0.10	0.09	0.10
Nickel	-0.01	-0.01	-0.01	0.25	0.26	0.25	0.25	0.25	0.25	0.14	0.19	0.14
Zinc	-0.00	-0.01	-0.00	0.25	0.16	0.24	0.25	0.15	0.24	0.12	0.11	0.12

Table 7.3 shows the results of cross-validation after backtransformation to the original scale (see Section 4.5, Eq. (4.3)). The ME at the original scale indicates that concentrations are in general systematically underestimated. The SDE values in Table 7.3 indicate that concentrations of Arsenic and Lead are predicted more precisely for the German part of the study area than for the Dutch part. However, predictions of concentrations of Cadmium, Copper, Nickel and Zinc appear to be relatively precise in the Dutch part. The RMSE values in Table 7.3 indicate that concentrations of Arsenic and Lead are predicted relatively accurate for the German part of the study area. However, the RMSE indicates that predictions of Cadmium, Copper, Nickel and Zinc concentrations are relatively inaccurate in the German part. The MEDAE values in Table 7.3 indicate that concentrations of Arsenic and Copper are predicted relatively accurate at the original scale in the German part of the study area. The mean of the absolute errors (MAE) indicate relatively accurate predictions for Arsenic and Copper in Germany.

Table 7.3. Results of cross-validation after backtransformation to the original scale. ME=mean error, SDE=standard deviation of error, RMSE=root mean squared error, MEDAE=median absolute error, MAE=mean absolute error. D=Germany, NL=The Netherlands

Heavy	ME			SDE			RMSE			MEDAE		
metal	D	NL	tot.	D	NL	tot.	D	NL	tot.	D	NL	tot.
Arsenic	1.58	2.99	1.70	8.53	9.84	8.65	8.67	10.17	8.80	1.45	2.20	1.49
Cadmium	0.02	0.02	0.02	0.21	0.11	0.20	0.21	0.11	0.20	0.08	0.05	0.08
Copper	1.32	2.43	1.38	9.08	7.64	9.01	9.17	7.92	9.11	2.54	3.88	2.54
Lead	0.74	1.93	0.81	12.31	13.52	12.37	12.32	13.49	12.39	4.50	3.33	4.48
Nickel	0.54	0.76	0.55	4.98	3.49	4.91	5.00	3.53	4.93	1.44	1.38	1.42
Zinc	1.05	-0.85	0.94	24.49	13.34	24.01	24.50	13.21	24.02	9.42	5.77	9.00

Heavy	MAE		
metal	D	NL	tot.
Arsenic	3.90	5.06	4.00
Cadmium	0.13	0.07	0.12
Copper	4.91	5.66	4.95
Lead	7.55	7.23	7.54
Nickel	2.74	2.14	2.70
Zinc	14.75	9.00	14.44

Chapter 8

Conclusions

1. Despite the fact that heavy metal concentrations are much more densely observed in Germany than in the Netherlands, the maps of heavy metal concentrations generally do not show pronounced discontinuities along the border;

2. Cross-validation generally does not indicate large differences in accuracy of spatial predictions between the German and Dutch part of the study area. However, it should be noted that the number of cross validation locations in the Dutch part is low and locations are clustered, which may result in inaccurate estimates of prediction errors;

3. The maps of prediction error variance at a logarithmic scale show a clear discontinuity along the border: large prediction error variances in the Dutch part, small prediction error variances in the German part. This is mainly explained by the kriging variance, which reflects the differences in density of observation points between the Dutch and the German part;

4. Lack of observed heavy metal concentrations in the Dutch part is compensated by relatively detailed ancillary information, resulting in maps without discontinuities along the German-Dutch border with respect to interpolated values. However, the variance of prediction errors at a logarithmic scale is much larger in the Dutch part than in the German part, indicating that the predictions in the Dutch part are relatively inaccurate;

5. We recommend that the results at a logarithmic scale are the basis for maps indicating the risks that critical levels are exceeded, since at the logarithmic scale assumptions on normality of the distributions of the predictions are not needed.

Bibliography

Benzler, J.-H., Finnern, H., Müller, W., Roeschmann, G., Will, K., and Wittmann, O., editors (1982). *Bodenkundliche Kartieranleitung*. AG Bodenkunde, Hannover.

Brus, D., Knotters, M., Van Dooremolen, W., Van Kernebeek, P., and Van Seeters, R. (1992). The use of electromagnetic measurements of apparent soil electrical conductivity to predict the boulder clay depth. *Geoderma*, 55:79–93.

De Oliveira, V. (2006). On optimal point and block prediction in log-gaussian random fields. *Scandinavian Journal of Statistics*, 33:523–540.

Deutsch, C. and Journel, A. (1998). *GSLIB. Geostatistical Software Library and User's Guide*. Oxford University Press, New York.

Dworschak, M., Schrey, H.-P., and Schulte-Kellinghaus, S. (2001). *Allgemeine Informationen zur Bodenkarte 1:50 000*. Geologischer Dienst Nordrhein-Westfalen, Krefeld.

Harbers, P. and Rosing, H. (1983). *Bodemkaart van Nederland Schaal 1:50 000. Toelichting bij de kaartbladen 41 West Aalten en 41 Oost Aalten*. Stichting voor Bodemkartering, Wageningen.

Journel, A. and Huijbregts, C. J. (1978). *Mining geostatistics*. Academic Press, London.

Stiboka (1975). *Bodemkaart van Nederland Schaal 1:50 000. Toelichting bij de kaartbladen 40 West Arnhem en 40 Oost Arnhem*. Stichting voor Bodemkartering, Wageningen.

Van der Pouw, B. and Finke, P. (1999). Development and perspective of soil survey in the Netherlands. In Bullock, P., Jones, R., and Montanarella, L., editors, *Soil resources of Europe. European Soil Bureau research report 6*. Office for Official Publications of the European Communities, Luxembourg.

Appendix A

Ancillary information

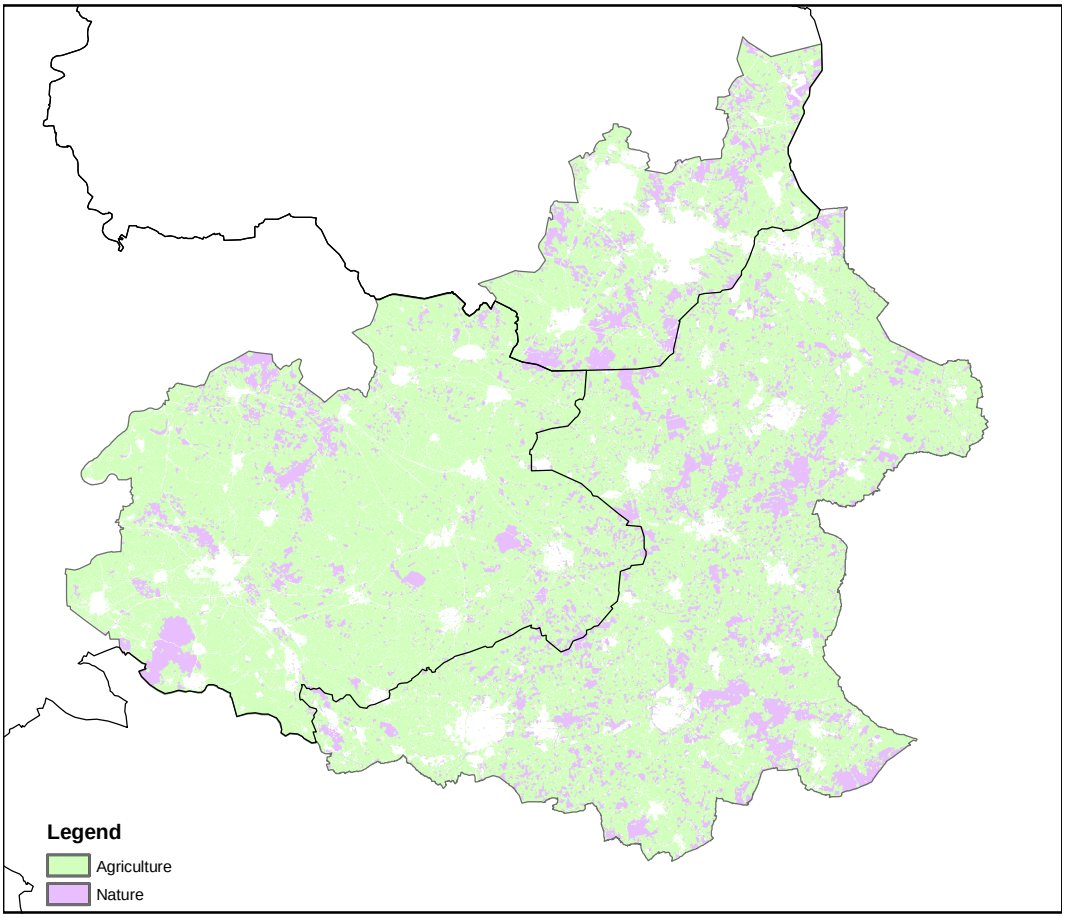

Figure A.1. Map of land use

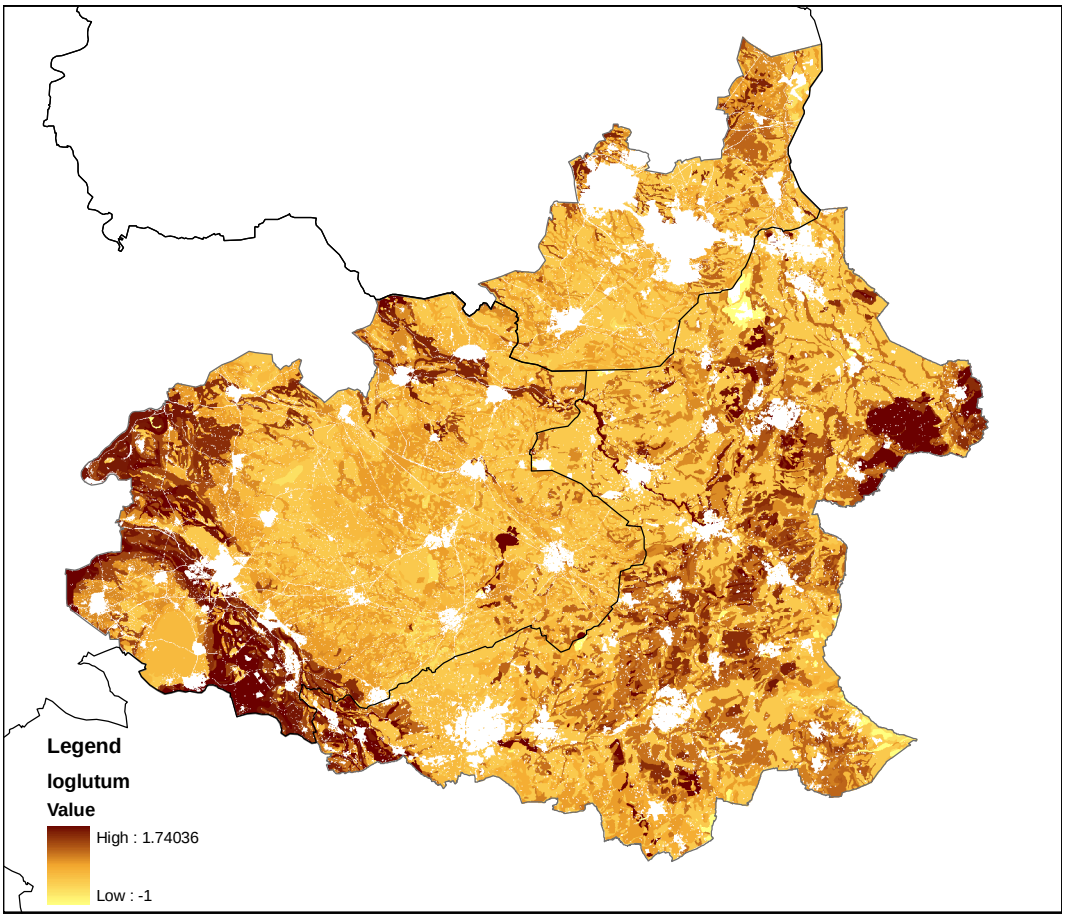

Figure A.2. Map of clay content (after logarithmic transformation)

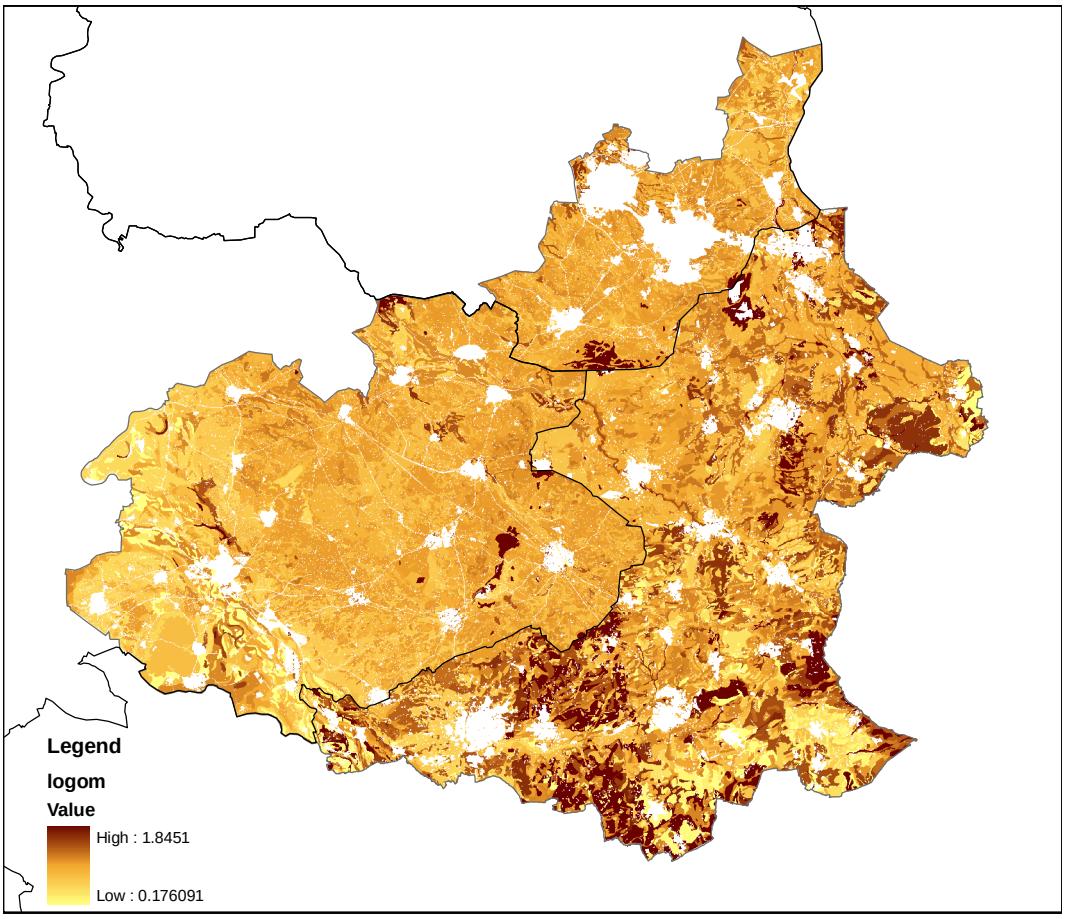

Figure A.3. Map of organic matter content (after logarithmic transformation)

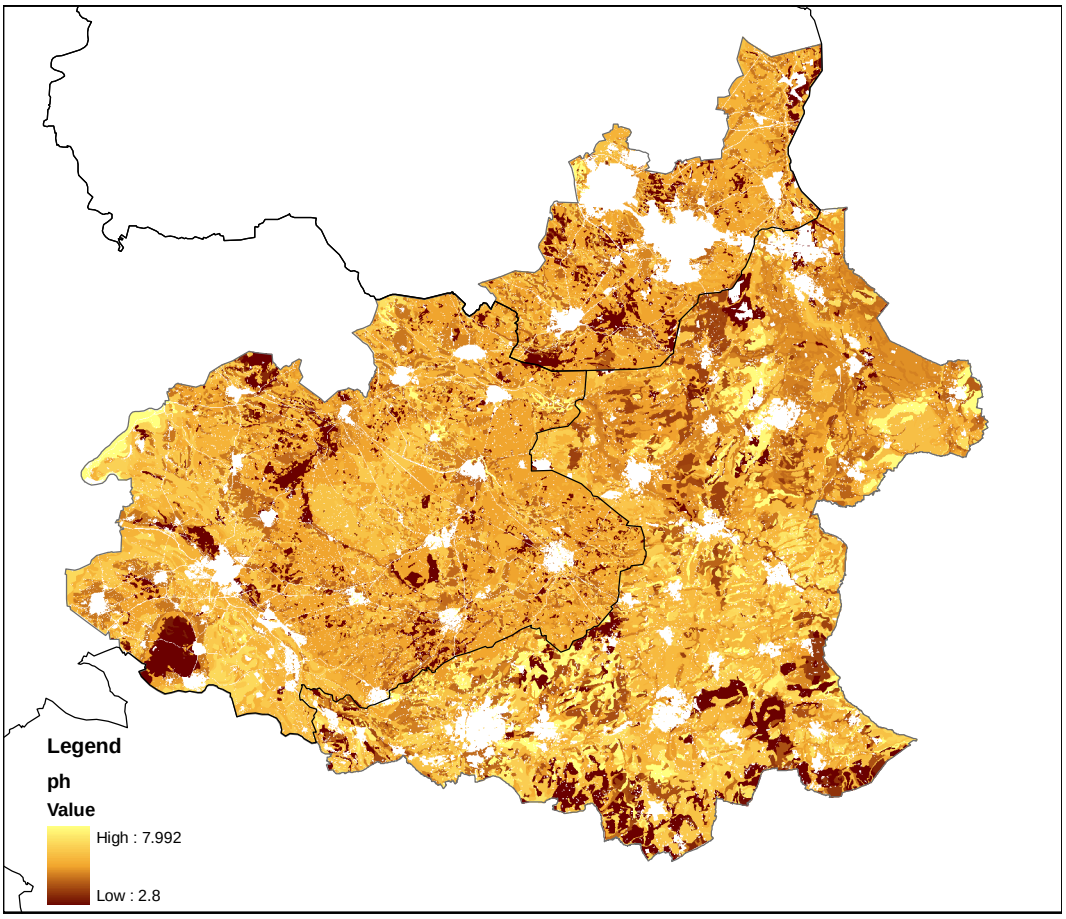

Figure A.4. Map of $pH_{\mathrm{CaCl_2}}$

Appendix B

Scheme of interpolation procedure

B.1 Procedure of spatial interpolation

Deterministic predictions of concentrations of Arsenic from ancillary information (at logarithmic scale) + interpolated residuals:

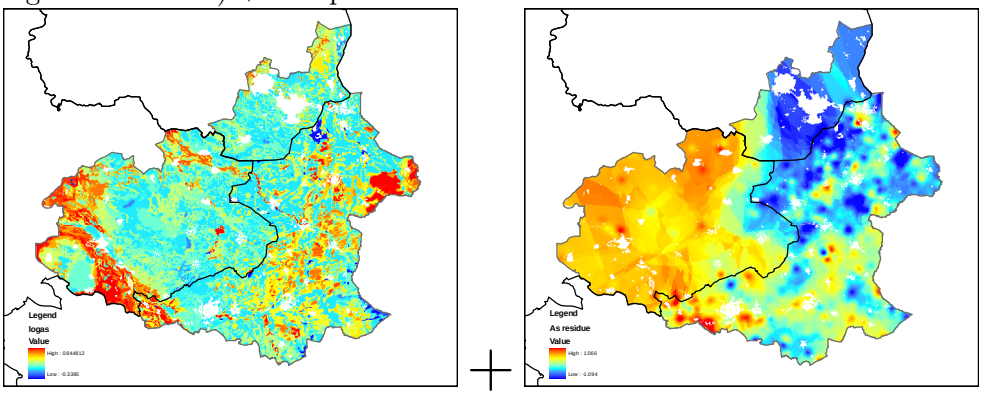

=

Interpolated values of concentrations of Arsenic (at logarithmic scale):

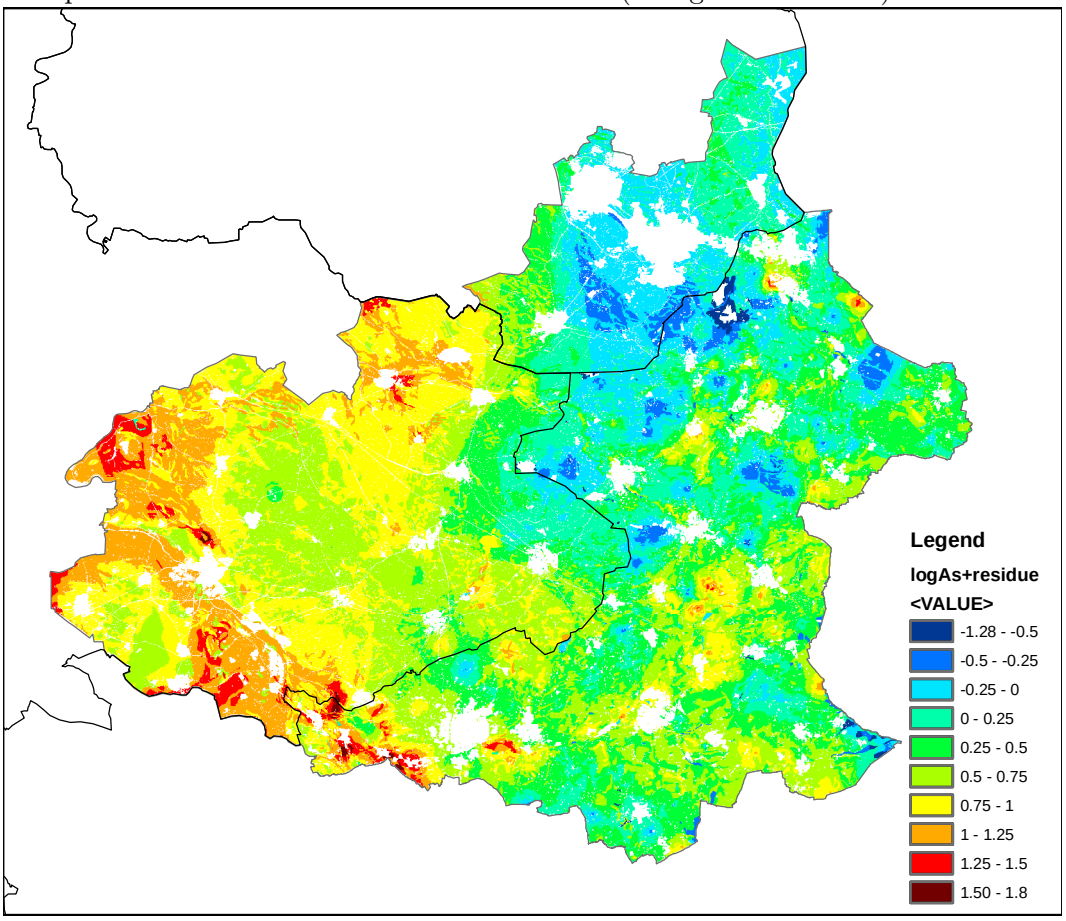

B.2 Procedure of mapping accuracy

Variance of the expected value of (logarithmically transformed) concentrations of Arsenic, $\sigma^2\{\mathrm{E}z(\mathbf{u}_j)\}$ + variance of kriged residuals:

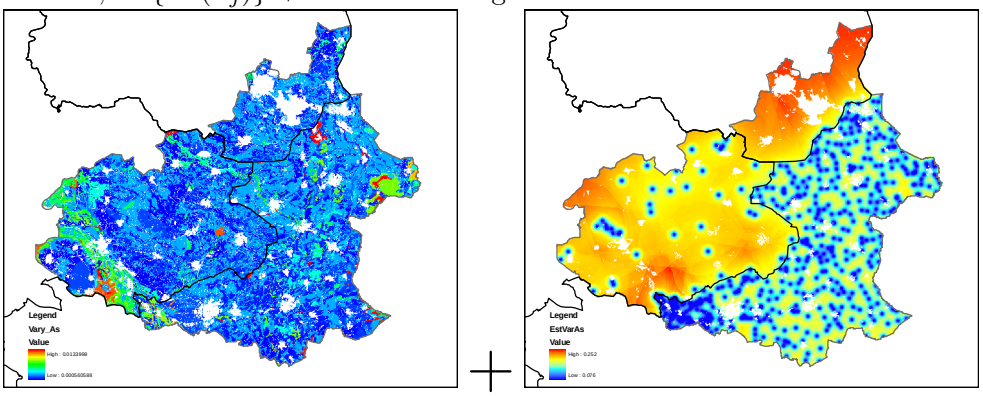

=

Variance of interpolation errors of concentrations of Arsenic (at logarithmic scale):

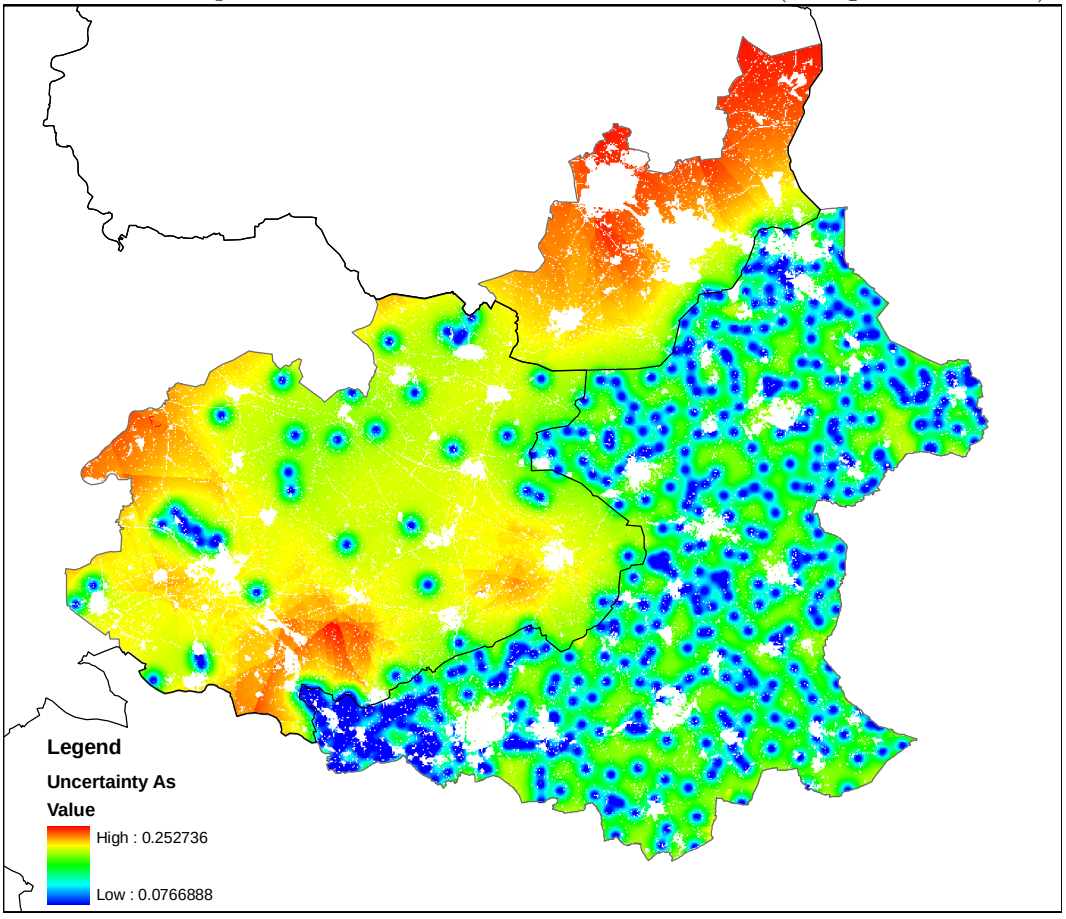

Appendix C

Results of regression

C.1 Model of Arsenic

Model (3.3) was calibrated to the data of As by applying the procedure described in Section 3.2. The left detection limit is equal to 0.3 mg/kg. The calibrated parameter values and their approximated standard errors are listed below:

	estimate	"s.e."
$\hat{b}_0$	-0.002	0.244
$\hat{b}_1$, nature	0.009	0.112
$\hat{b}_2$, $\log 10(CC)$	0.5113	0.0719
$\hat{b}_3$, $\log 10(OM)$	0.122	0.122
$\hat{b}_4$, pH	0.0020	0.0413
s	0.5475	0.0186

The percentage of variance accounted for is estimated at 11.3 %. Next, the model was re-estimated after dropping the non-significant terms, resulting in the following parameter estimates:

	estimate	"s.e."
$\hat{b}_0$	0.1298	0.0569
$\hat{b}_2$, $\log 10(CC)$	0.4683	0.0630
s	0.5525	0.0182

The percentage of variance accounted for is estimated at 9.7 %. A maximum-likelihood estimate of values below the detection limit is 0.1789 mg/kg.

C.2 Models for natural areas including forests

C.2.1 Model of Cadmium

Model (3.1) was calibrated to the data of Cd by applying the procedure described in Section 3.2. The left detection limit is equal to 0.04 mg/kg. The calibrated parameter values and their approximated standard errors are listed below:

	estimate	"s.e."
$\hat{b}_0$	-3.626	0.205
$\hat{b}_1$, $\log 10(CC)$	-0.254	0.262
$\hat{b}_2$, $\log 10(OM)$	1.387	0.423
$\hat{b}_3$, pH	0.4754	*
s	0.3981	0.0381

The percentage of variance accounted for is estimated at 59.4 %. Next, the model was re-estimated after dropping the non-significant terms, resulting in the following parameter estimates:

	estimate	"s.e."
$\hat{b}_0$	-3.448	0.375
$\hat{b}_2$, $\log 10(OM)$	1.218	0.187
$\hat{b}_3$, pH	0.4101	0.0939
s	0.4444	0.0402

The percentage of variance accounted for is estimated at 49.4 %. A maximum-likelihood estimate of values below the detection limit is 0.01631 mg/kg.

C.2.2 Model of Copper

Model (3.1) was calibrated to the data of Cu. The calibrated parameter values and their approximated standard errors are listed below:

	estimate	s.e.	t-value (98 d.f.)
$\hat{b}_0$	-0.011	0.285	-0.04
$\hat{b}_1$, $\log 10(CC)$	0.3973	0.0904	4.39
$\hat{b}_2$, $\log 10(OM)$	0.473	0.147	3.22
$\hat{b}_3$, pH	0.0406	0.0743	0.55

The percentage of variance accounted for is estimated at 27.7 %. Next, the model was re-estimated after dropping the non-significant terms, resulting in the following parameter estimates:

	estimate	s.e.	t-value (99 d.f.)
$\hat{b}_0$	0.129	0.125	1.04
$\hat{b}_1$, $\log 10(CC)$	0.4060	0.0887	4.57
$\hat{b}_2$, $\log 10(OM)$	0.454	0.142	3.19

The percentage of variance accounted for is estimated at 28.2 %.

C.2.3 Model of Lead

Model (3.1) was calibrated to the data of Pb. The calibrated parameter values and their approximated standard errors are listed below:

	estimate	s.e.	t-value (98 d.f.)
$\hat{b}_0$	1.065	0.139	7.65
$\hat{b}_1$, $\log 10(CC)$	0.2432	0.0442	5.50
$\hat{b}_2$, $\log 10(OM)$	0.6543	0.0718	9.11
$\hat{b}_3$, pH	-0.0621	0.0363	-1.71

The percentage of variance accounted for is estimated at 61.6 %. Next, the model was re-estimated after dropping the non-significant terms, resulting in the following parameter estimates:

	estimate	s.e.	t-value (99 d.f.)
$\hat{b}_0$	0.8510	0.0617	13.80
$\hat{b}_1$, $\log 10(CC)$	0.2302	0.0440	5.23
$\hat{b}_2$, $\log 10(OM)$	0.6835	0.0704	9.70

The percentage of variance accounted for is estimated at 60.9 %.

C.2.4 Model of Nickel

Model (3.1) was calibrated to the data of Ni. The calibrated parameter values and their approximated standard errors are listed below:

	estimate	s.e.	t-value (95 d.f.)
$\hat{b}_0$	-0.358	0.228	-1.57
$\hat{b}_1$, $\log 10(CC)$	0.4295	0.0734	5.85
$\hat{b}_2$, $\log 10(OM)$	0.286	0.118	2.42
$\hat{b}_3$, pH	0.1281	0.0596	2.15

The percentage of variance accounted for is estimated at 36.3 %.

C.2.5 Model of Zinc

Model (3.1) was calibrated to the data of Zn. The calibrated parameter values and their approximated standard errors are listed below:

	estimate	s.e.	t-value (98 d.f.)
$\hat{b}_0$	-0.638	0.194	-3.28
$\hat{b}_1$, $\log 10(CC)$	0.3215	0.0617	5.21
$\hat{b}_2$, $\log 10(OM)$	0.669	0.100	6.67
$\hat{b}_3$, pH	0.3428	0.0507	6.76

The percentage of variance accounted for is estimated at 57.4 %.

C.3 Models for agricultural land

C.3.1 Model of Cadmium

Model (3.1) was calibrated to the data of Cd by applying the procedure described in Section 3.2. The left detection limit is equal to 0.04 mg/kg. The calibrated parameter values and their approximated standard errors are listed below:

	estimate	"s.e."
$\hat{b}_0$	-1.417	0.170
$\hat{b}_1$, $\log 10(CC)$	-0.0602	0.0602
$\hat{b}_2$, $\log 10(OM)$	0.4550	0.0996
$\hat{b}_3$, pH	0.1026	0.0295
s	0.3153	0.0124

The residual variance exceeds the variance of the response variate. Next, the model was re-estimated after dropping the non-significant terms, resulting in the following parameter estimates:

	estimate	"s.e."
$\hat{b}_0$	-1.4076	0.0735
$\hat{b}_2$, $\log 10(OM)$	0.7286	0.0276
$\hat{b}_3$, pH	0.0727	0.0128
s	0.16985	0.00609

The percentage of variance accounted for is estimated at 60.0 %. A maximum-likelihood estimate of values below the detection limit is 0.03379 mg/kg.

C.3.2 Model of Copper

Model (3.1) was calibrated to the data of Cu. The calibrated parameter values and their approximated standard errors are listed below:

	estimate	s.e.	t-value (379 d.f.)
$\hat{b}_0$	0.662	0.147	4.50
$\hat{b}_1$, $\log 10(CC)$	0.1517	0.0474	3.20
$\hat{b}_2$, $\log 10(OM)$	0.1926	0.0792	2.43
$\hat{b}_3$, pH	0.0195	0.0252	0.77

The percentage of variance accounted for is estimated at 3.7 %. Next, the model was re-estimated after dropping the non-significant terms, resulting in the following parameter estimates:

	estimate	s.e.	t-value (388 d.f.)
$\hat{b}_0$	0.7654	0.0639	11.97
$\hat{b}_1$, $\log 10(CC)$	0.1598	0.0447	3.57
$\hat{b}_2$, $\log 10(OM)$	0.1896	0.0775	2.45

The percentage of variance accounted for is estimated at 3.8 %.

C.3.3 Model of Lead

Model (3.1) was calibrated to the data of Pb. The calibrated parameter values and their approximated standard errors are listed below:

	estimate	s.e.	t-value (379 d.f.)
$\hat{b}_0$	0.9538	0.0820	11.62
$\hat{b}_1$, $\log 10(CC)$	0.2297	0.0264	8.69
$\hat{b}_2$, $\log 10(OM)$	0.3387	0.0442	7.67
$\hat{b}_3$, pH	-0.0048	0.0141	-0.34

The percentage of variance accounted for is estimated at 24.9 %. Next, the model was re-estimated after dropping the non-significant terms, resulting in the following parameter estimates:

	estimate	s.e.	t-value (388 d.f.)
$\hat{b}_0$	0.9279	0.0357	25.98
$\hat{b}_1$, $\log 10(CC)$	0.2295	0.0250	9.19
$\hat{b}_2$, $\log 10(OM)$	0.3346	0.0433	7.73

The percentage of variance accounted for is estimated at 24.9 %.

C.3.4 Model of Nickel

Model (3.1) was calibrated to the data of Ni. The calibrated parameter values and their approximated standard errors are listed below:

	estimate	s.e.	t-value (372 d.f.)
$\hat{b}_0$	-0.076	0.122	-0.62
$\hat{b}_1$, $\log 10(CC)$	0.4468	0.0395	11.31
$\hat{b}_2$, $\log 10(OM)$	0.0677	0.0652	1.04
$\hat{b}_3$, pH	0.0683	0.0210	3.25

The percentage of variance accounted for is estimated at 31.6 %. Next, the model was re-estimated after dropping the non-significant terms, resulting in the following parameter estimates:

	estimate	s.e.	t-value (596 d.f.)
$\hat{b}_0$	-0.0201	0.0909	-0.22
$\hat{b}_1$, $\log 10(CC)$	0.4084	0.0318	12.84
$\hat{b}_3$, pH	0.0644	0.0168	3.84

The percentage of variance accounted for is estimated at 26.5 %.

C.3.5 Model of Zinc

Model (3.1) was calibrated to the data of Zn. The calibrated parameter values and their approximated standard errors are listed below:

	estimate	s.e.	t-value (379 d.f.)
$\hat{b}_0$	0.7912	0.0799	9.91
$\hat{b}_1$, $\log 10(CC)$	0.3139	0.0257	12.20
$\hat{b}_2$, $\log 10(OM)$	0.2293	0.0430	5.33
$\hat{b}_3$, pH	0.0759	0.0137	5.54

The percentage of variance accounted for is estimated at 39.5 %.

Appendix D

Results of spatial interpolation

D.1 Results at logarithmic scale

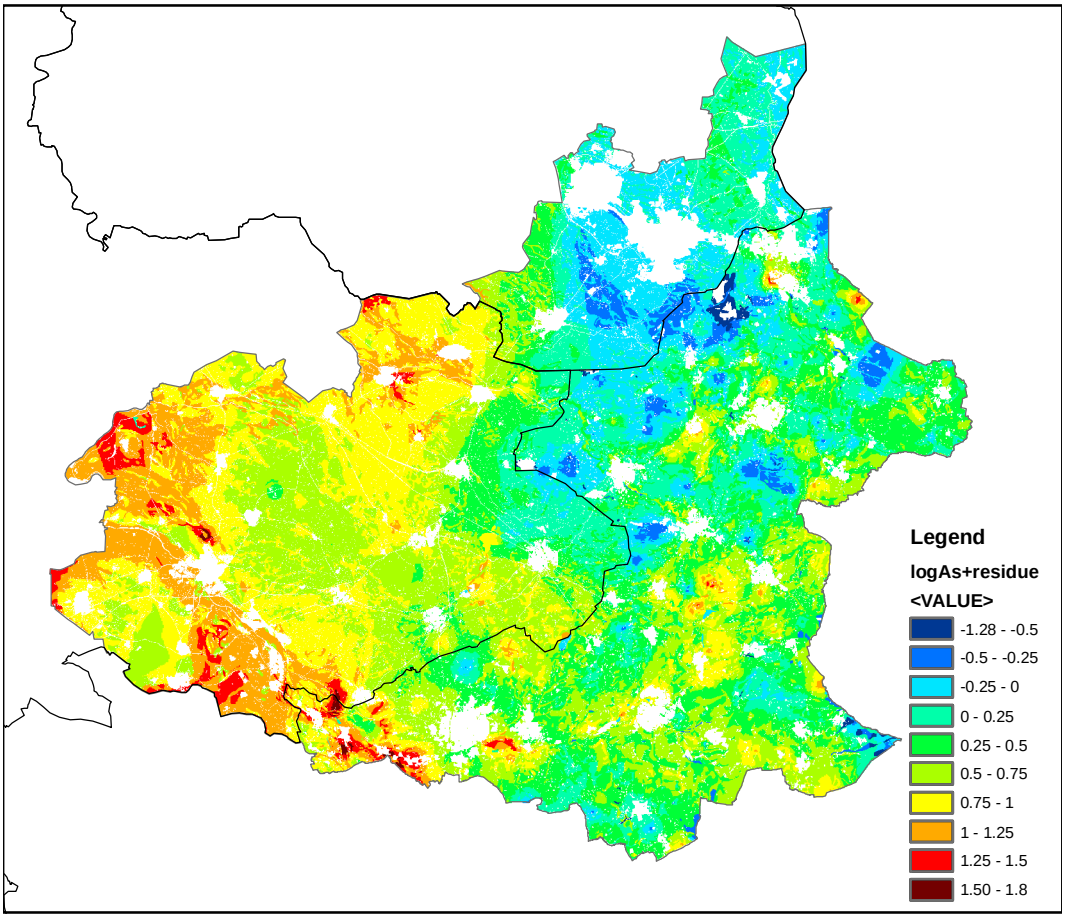

Figure D.1. Map of concentrations of Arsenic in the topsoil (at logarithmic scale)

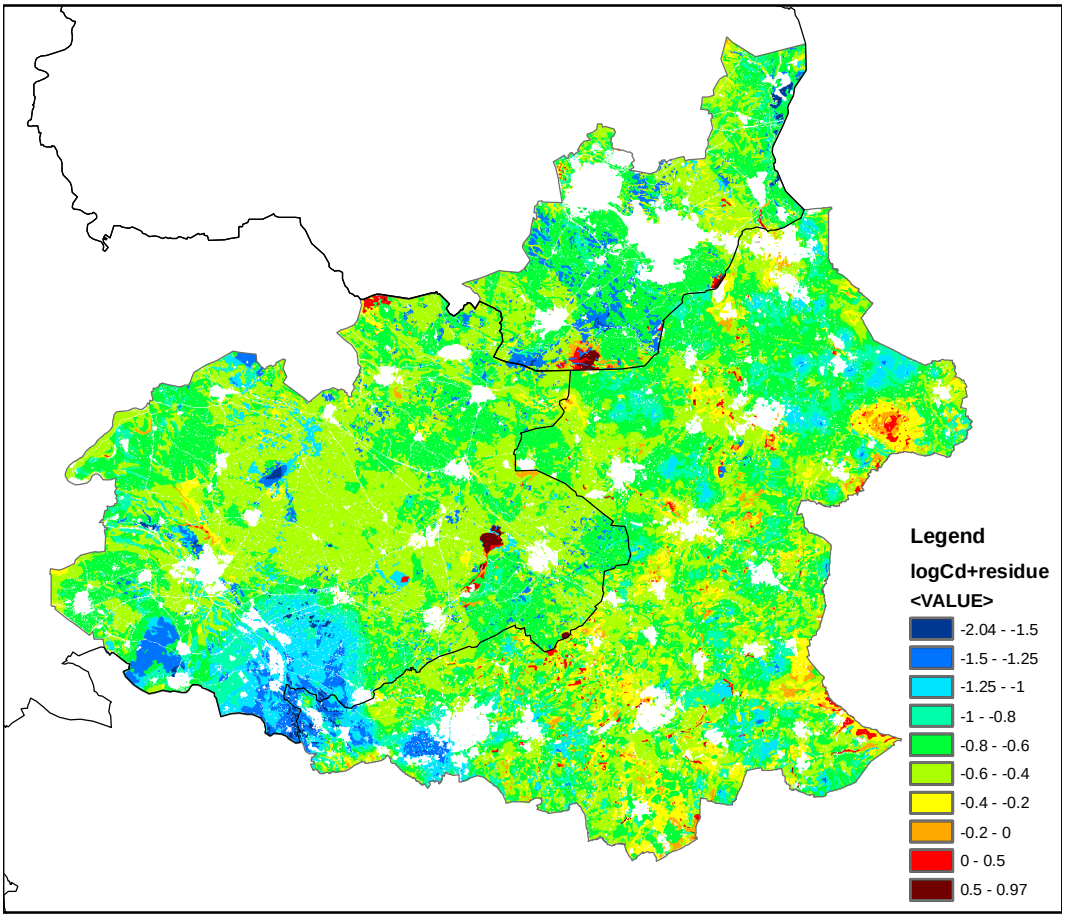

Figure D.2. Map of concentrations of Cadmium in the topsoil (at logarithmic scale)

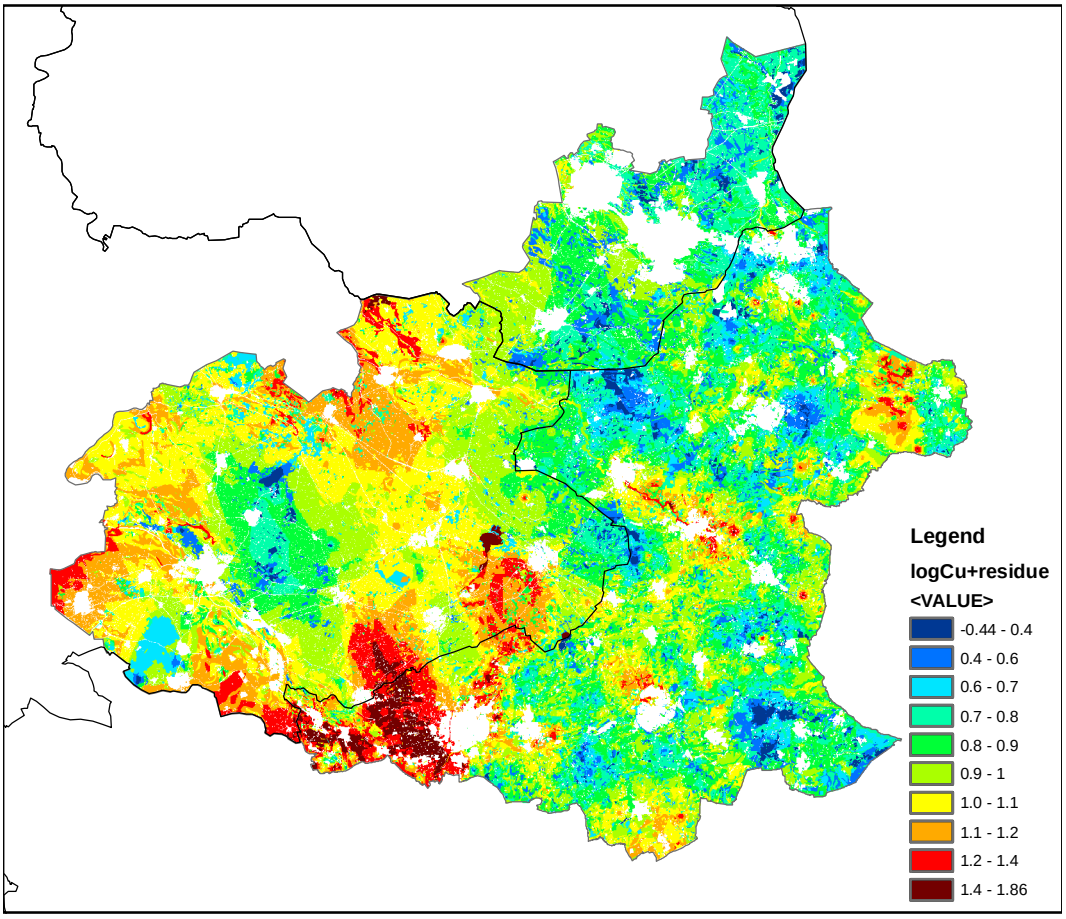

Figure D.3. Map of concentrations of Copper in the topsoil (at logarithmic scale)

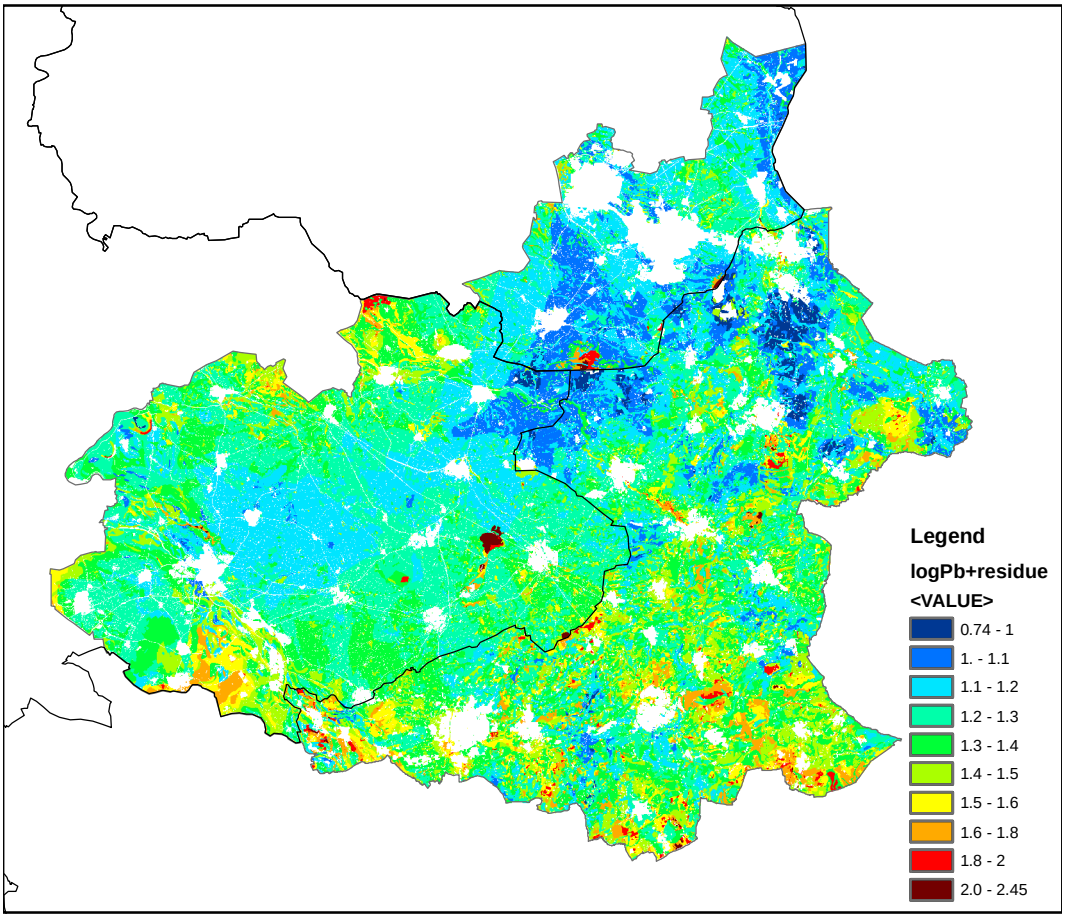

Figure D.4. Map of concentrations of Lead in the topsoil (at logarithmic scale)

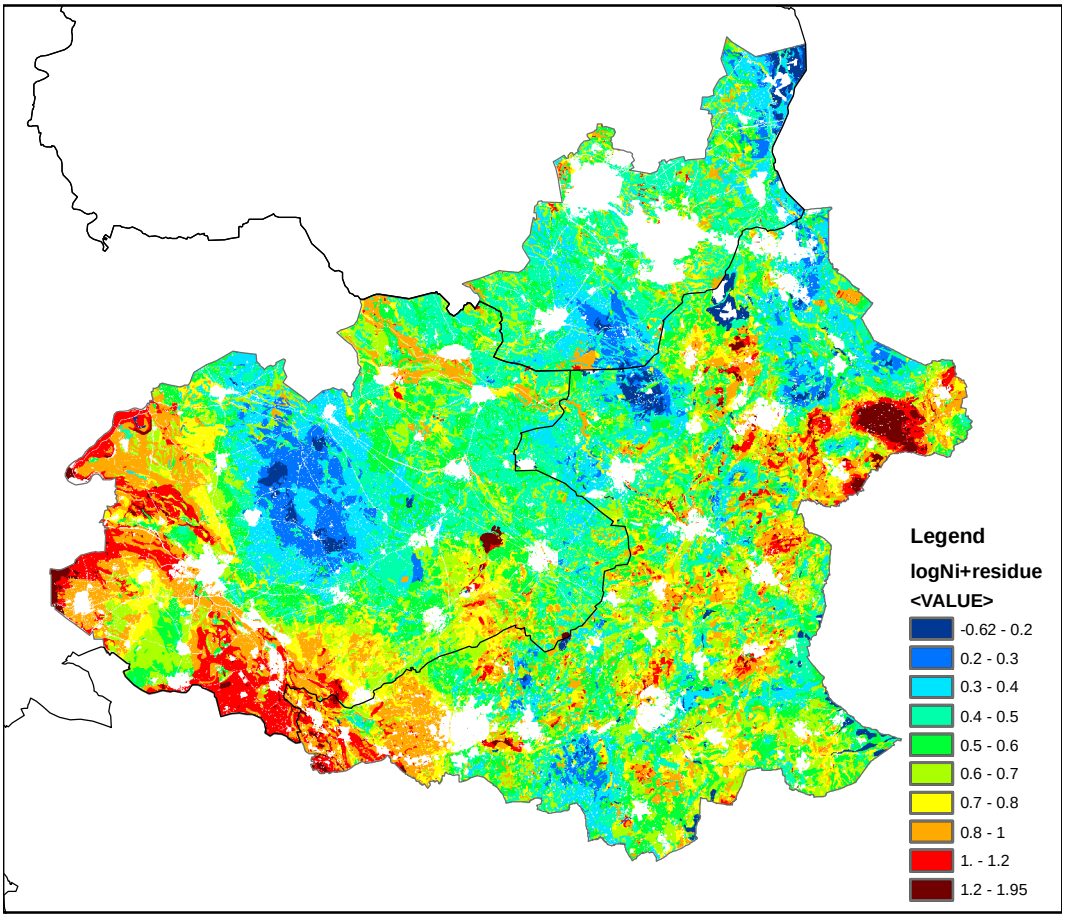

Figure D.5. Map of concentrations of Nickel in the topsoil (at logarithmic scale)

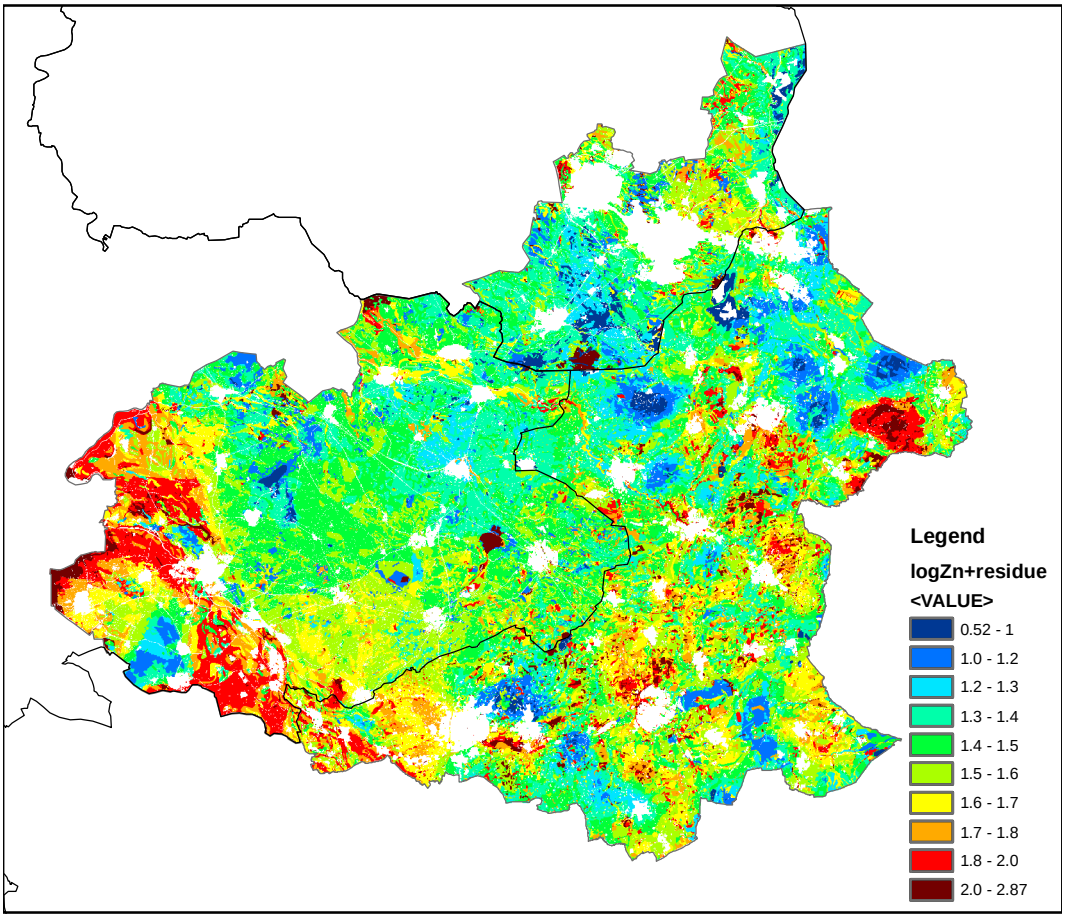

Figure D.6. Map of concentrations of Zinc in the topsoil (at logarithmic scale)

D.2 Results at original scale

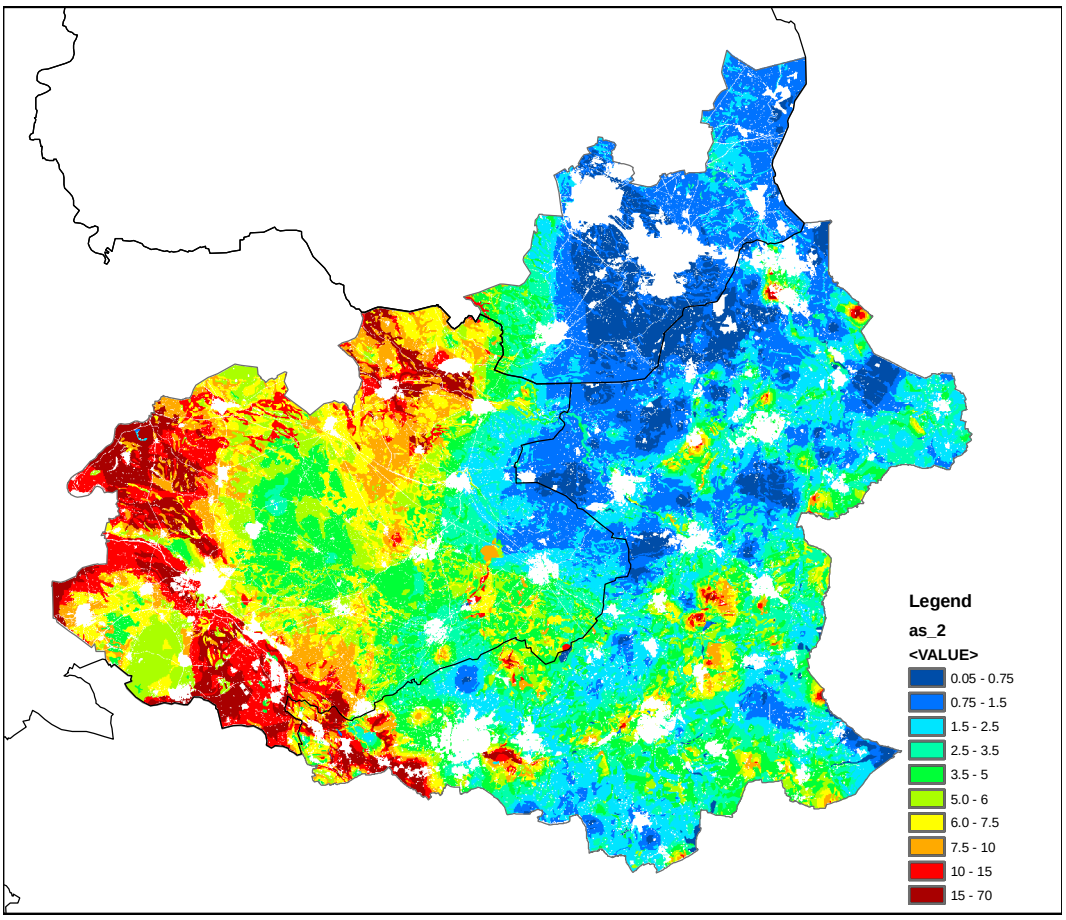

Figure D.7. Map of concentrations of Arsenic in the topsoil

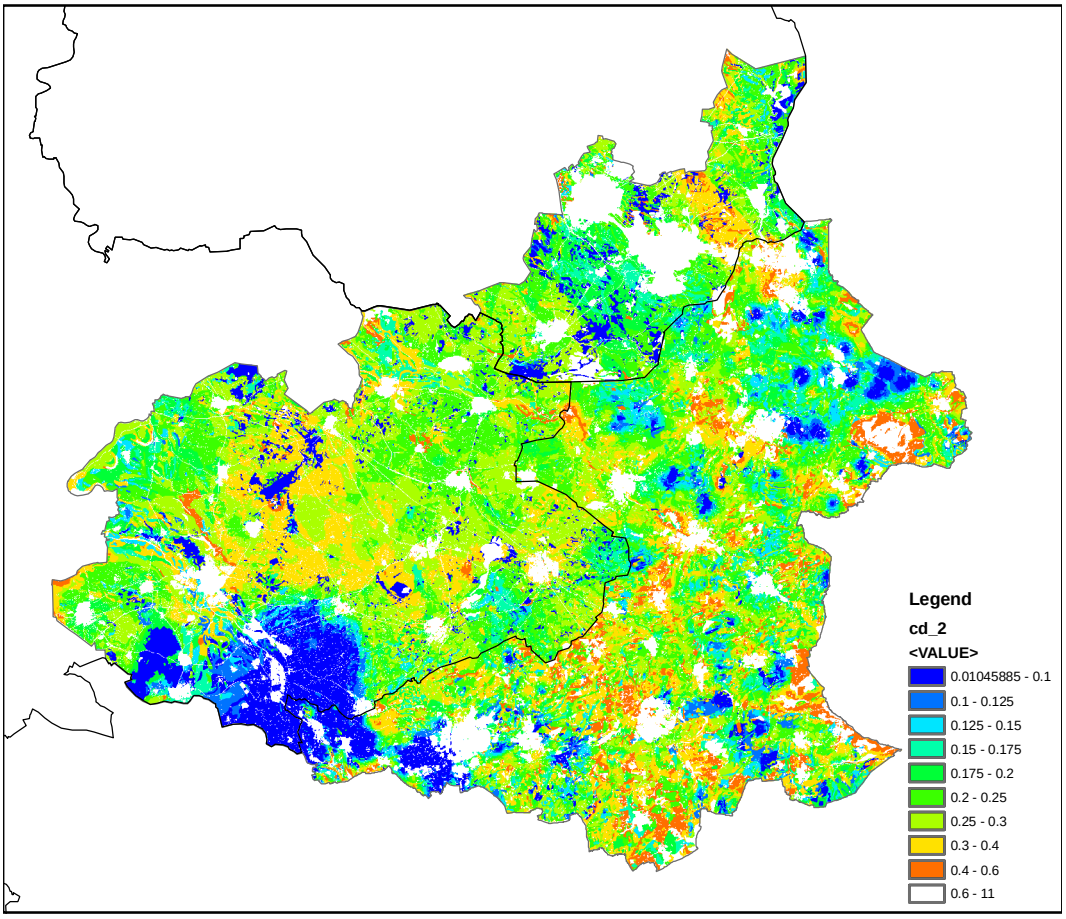

Figure D.8. Map of concentrations of Cadmium in the topsoil

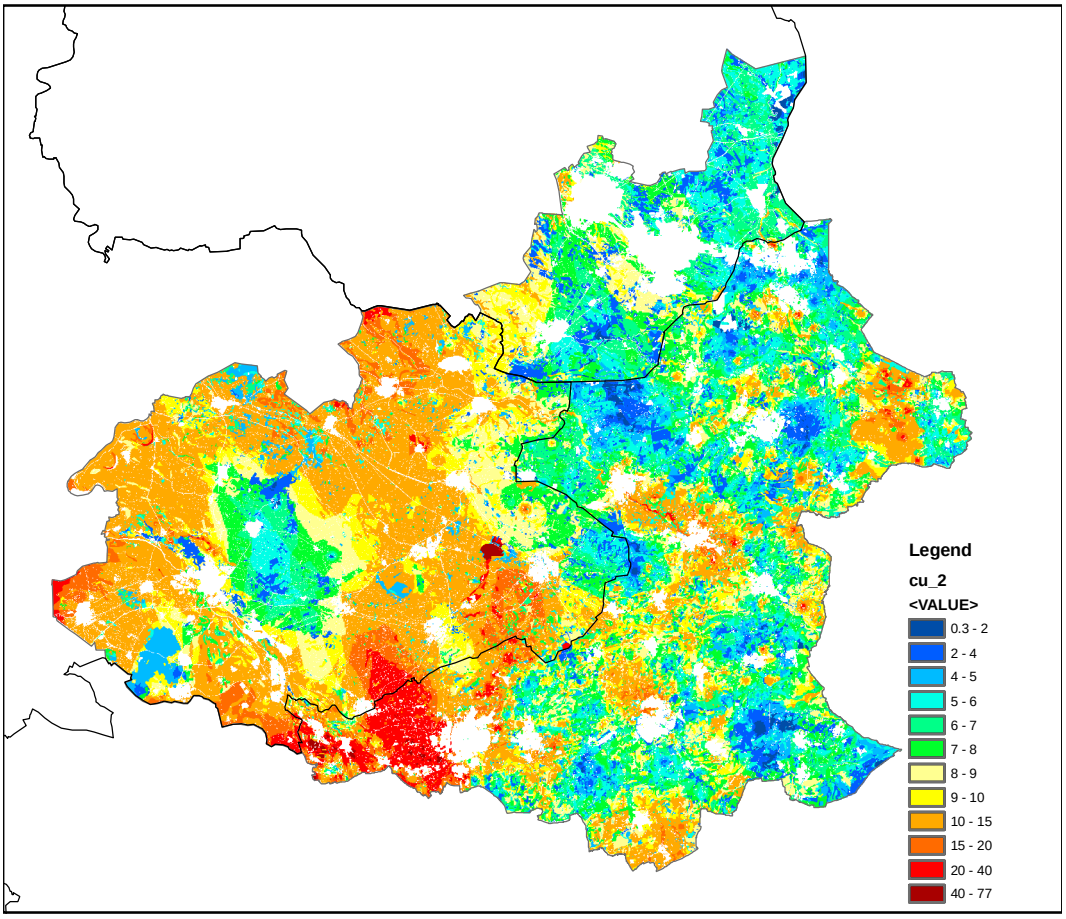

Figure D.9. Map of concentrations of Copper in the topsoil

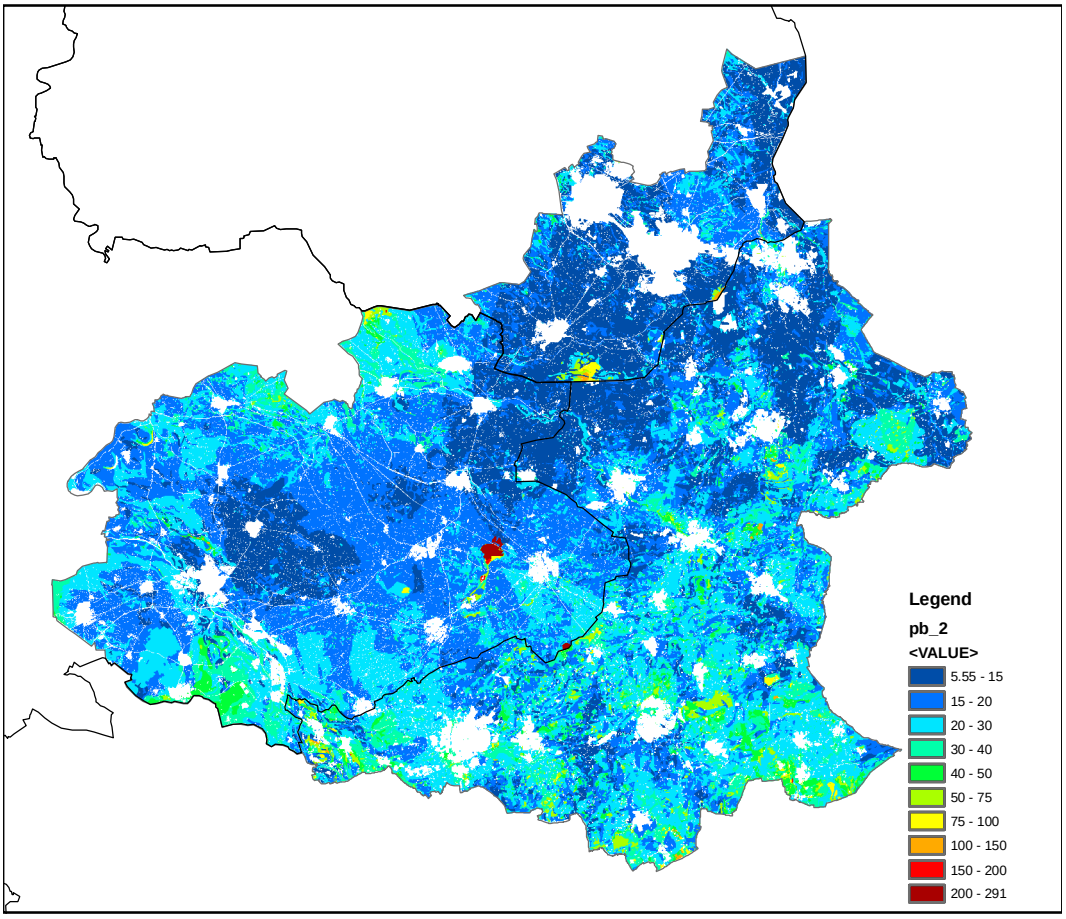

Figure D.10. Map of concentrations of Lead in the topsoil

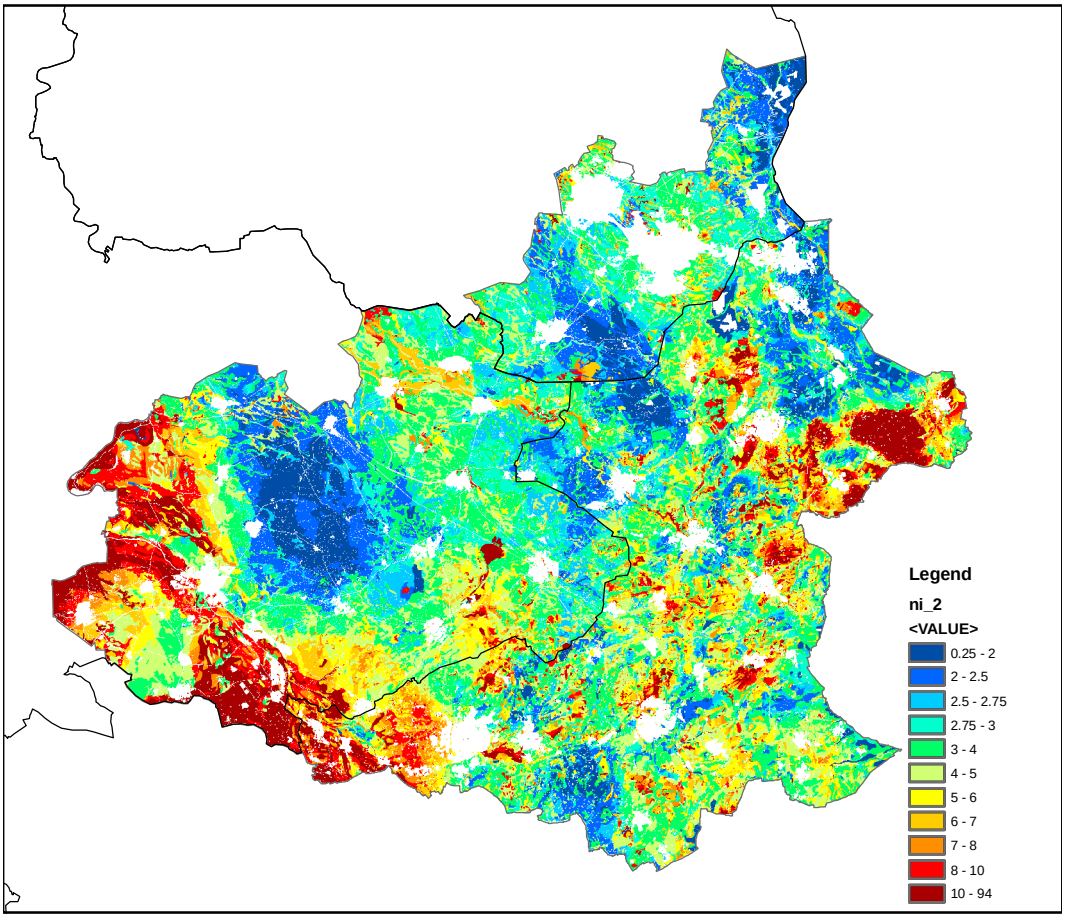

Figure D.11. Map of concentrations of Nickel in the topsoil

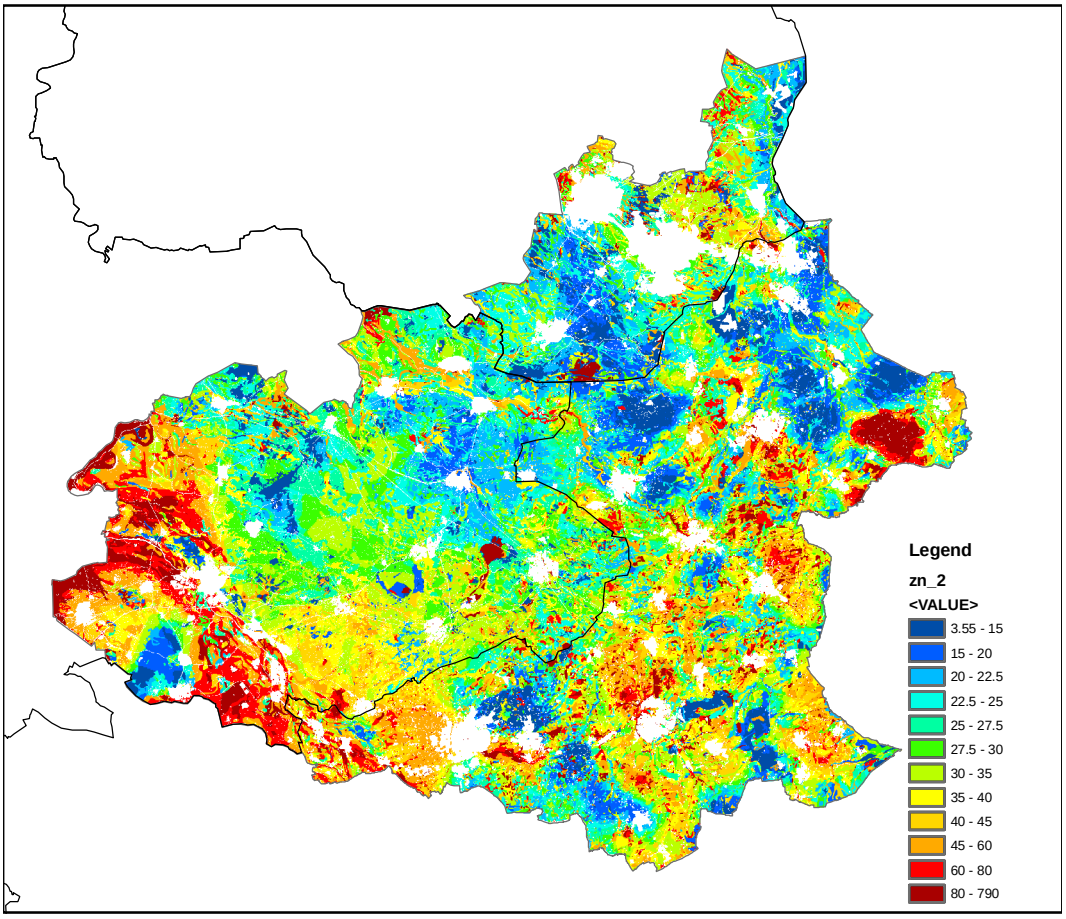

Figure D.12. Map of concentrations of Zinc in the topsoil

Appendix E

Accuracy of spatial predictions

E.1 Accuracy of predictions at logarithmic scale

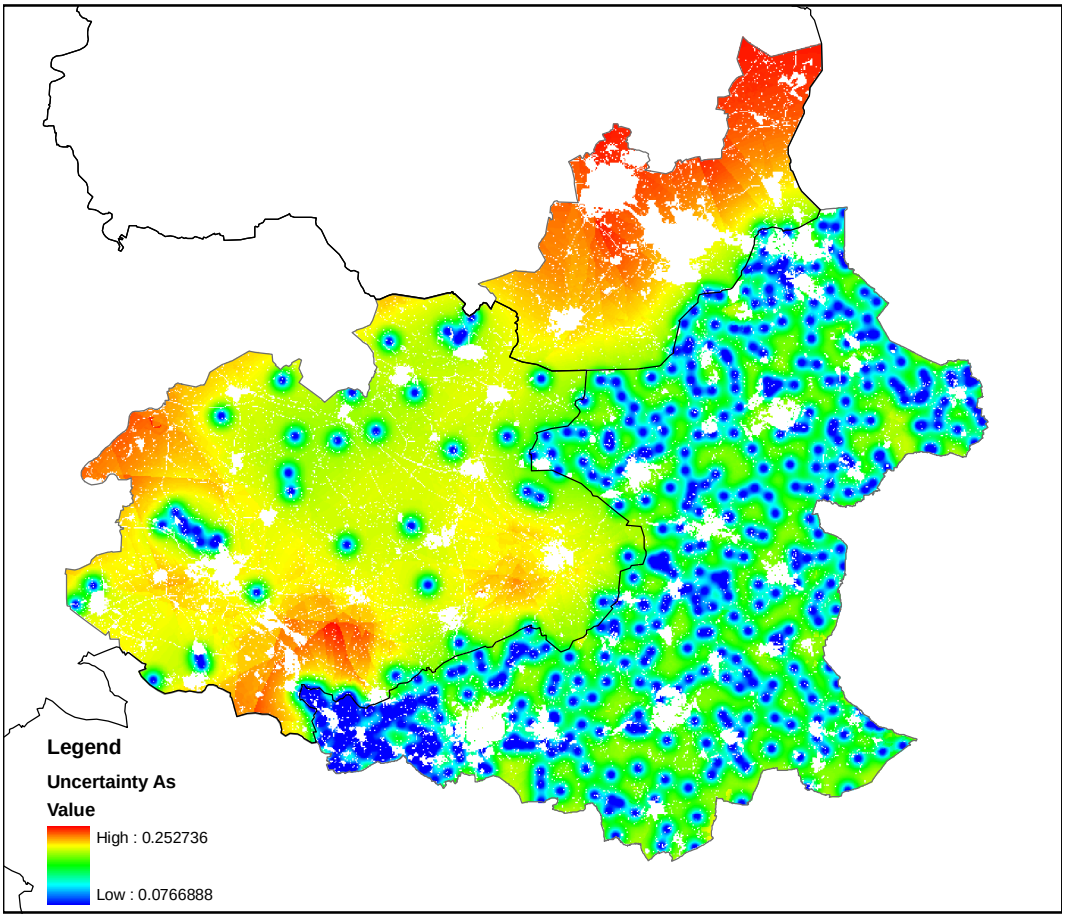

Figure E.1. Variance of interpolation errors for Arsenic

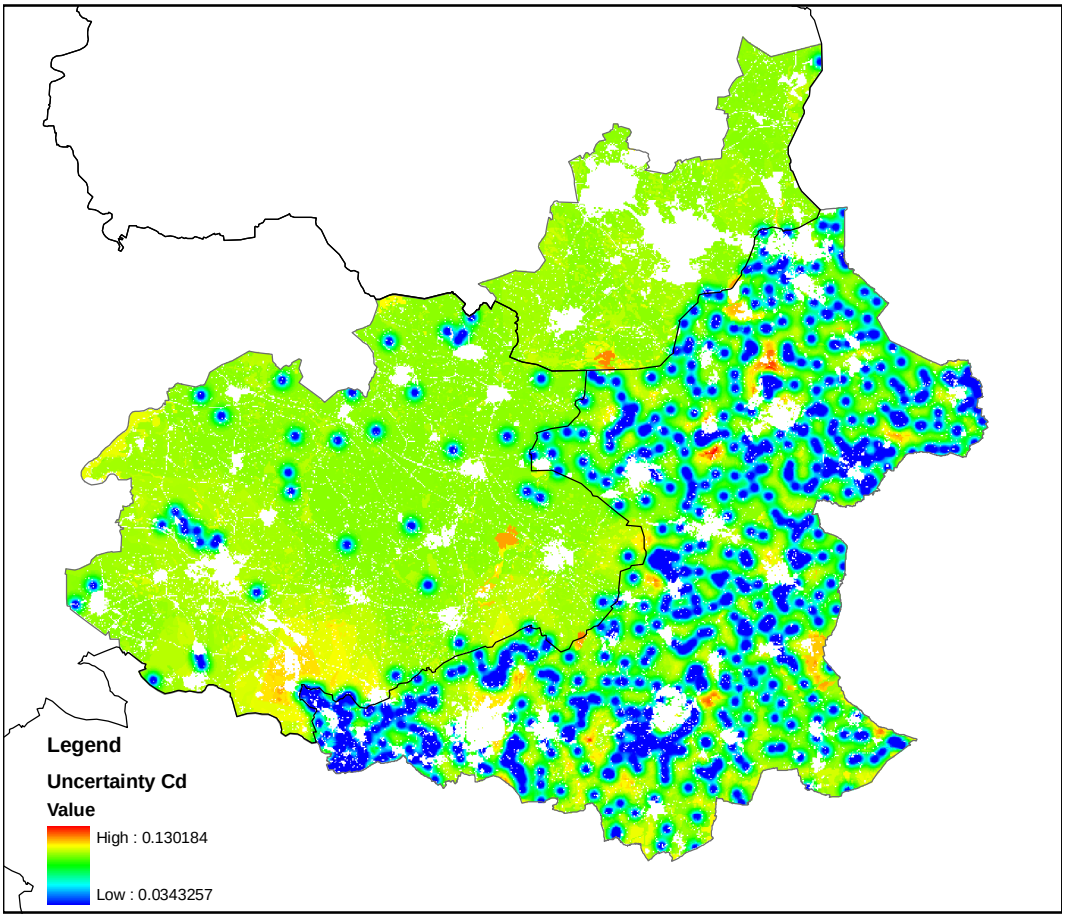

Figure E.2. Variance of interpolation errors for Cadmium

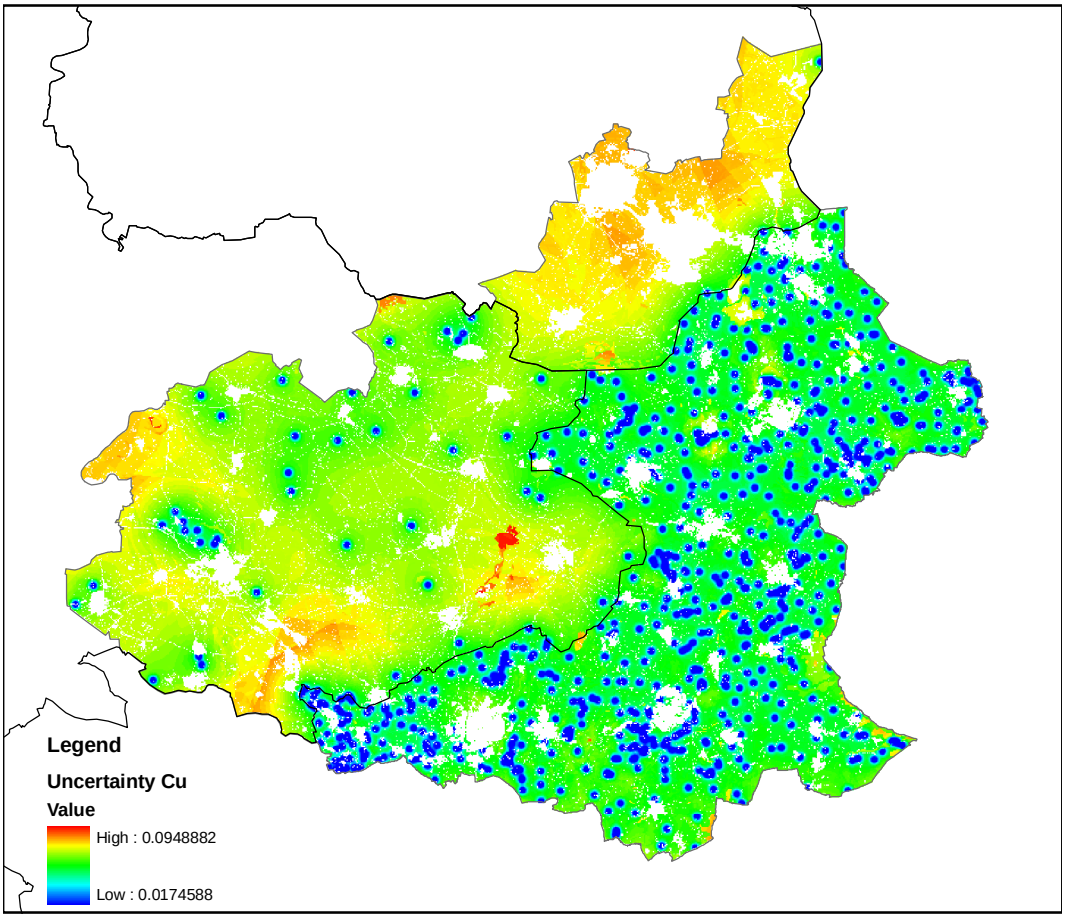

Figure E.3. Variance of interpolation errors for Copper

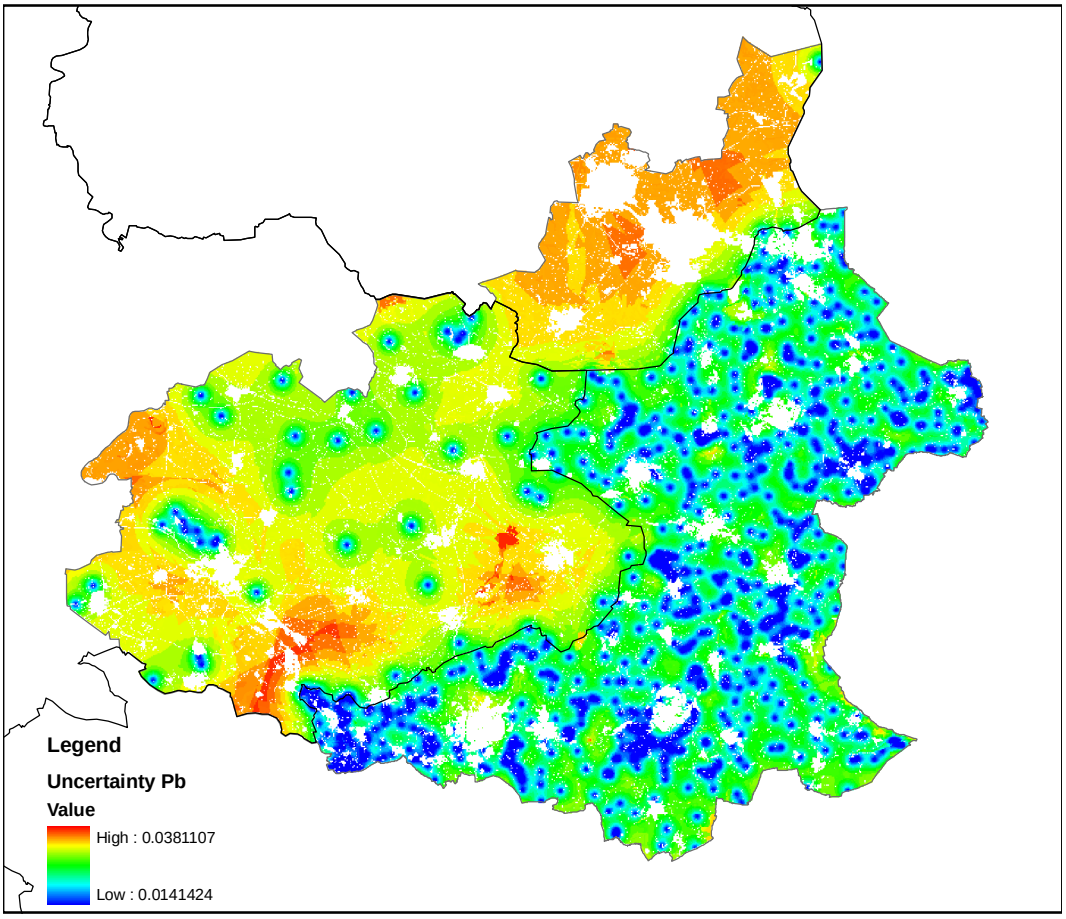

Figure E.4. Variance of interpolation errors for Lead

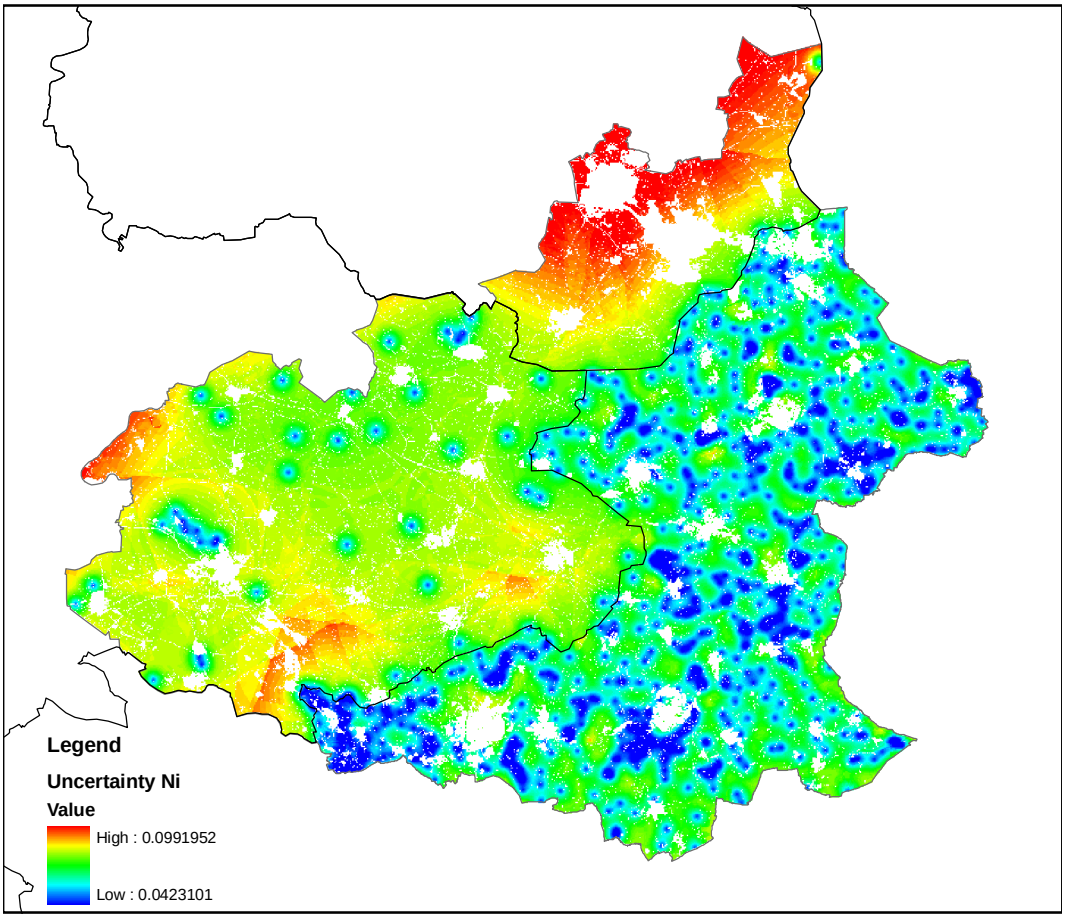

Figure E.5. Variance of interpolation errors for Nickel

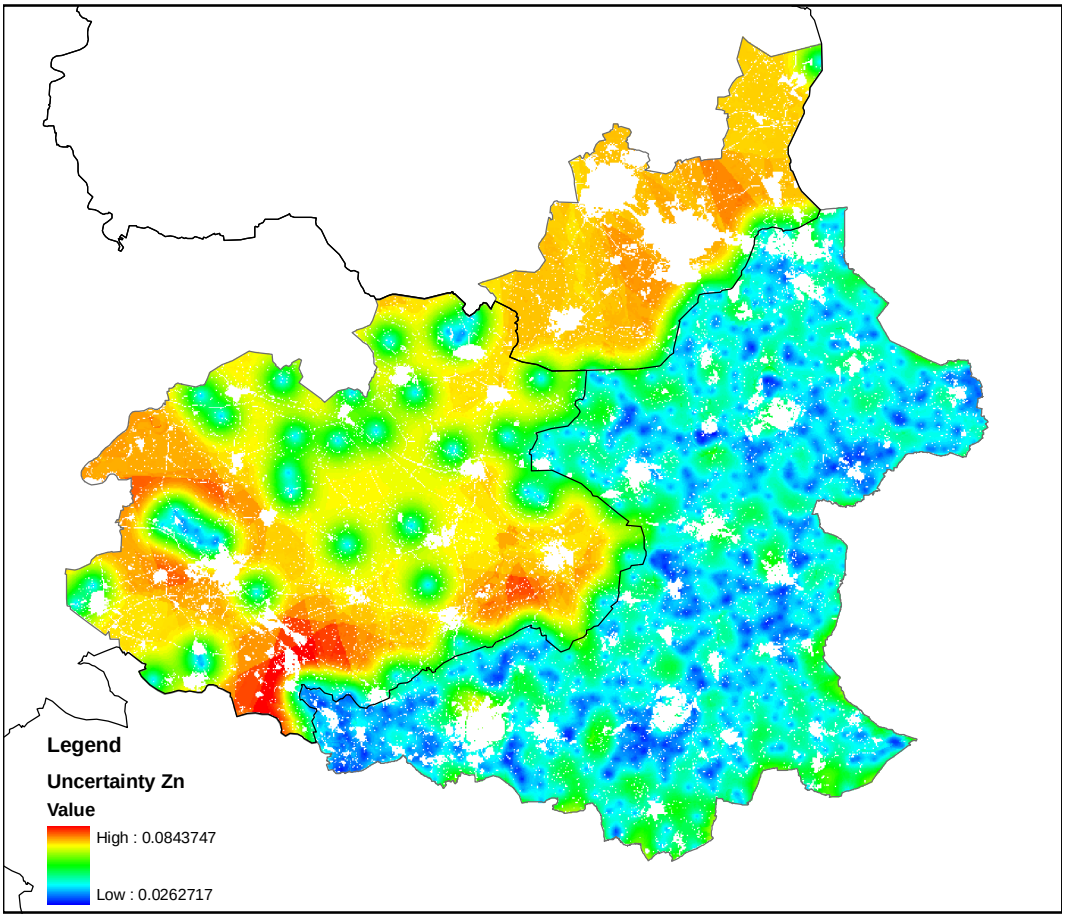

Figure E.6. Variance of interpolation errors for Zinc